Quantum Memory for Light

Jean-Louis Le Gouët

Quantum Memory for Light*

Jean-Louis Le Gouët
Laboratoire Aimé Cotton, CNRS UPR3321, Univ Paris Sud
bâtiment 505, campus universitaire, 91405 Orsay cedex
jean-louis.legouet@lac.u-psud.fr

Abstract

We ouline two strategies for storage and recovery of quantum light in an ensemble of atoms. This series of lectures has been devised as an elementary introduction. Hence discussion is essentially confined to a semi-classical picture. We first consider electromagnetically induced transparency (EIT) and stopped light. The roles of homogeneous and inhomogeneous broadening are examined. We propose both time- and frequency-domain descriptions. Then we discuss the total recall of a signal after capture by an absorbing material. Rephasing processes are briefly reviewed. We refer to various recent experimental works, especially those conducted in solid state media. The course is intended to be self contained and includes reminders on some quantum physics elements such as the density operator and the Bloch vector.

Contents

*This series of lectures was delivered at Ecole Prédoctorale des Houches, session XXIV, Quantum Optics, September 10-21, 2007. The session was directed by Nicolas Treps and Isabelle Robert-Philip.

1 Introduction

Transport of quantum information is ideally accomplished by light but, at some stage, a material system is needed for processing and/or storage. Many groups around the world strive to build a quantum memory that should store the non-classical properties of a light signal, then to restore the original signal. If long distance quantum cryptography is commonly invoked to justify these researches[1], above all this is a fascinating quantum physics problem, giving a new insight in light-matter interaction.

Quantum information is related to noise. When the fluctuations of a classical light source are reduced to the quantum limit, noise is equally distributed over a pair of conjugated observables such as photon number and phase, Stokes vector components or field quadratures. A light beam carries quantum information if the noise affecting one observable is squeezed under the standard quantum limit corresponding to equipartition of noise. Of course noise reduction on one observable entails increased noise on the conjugate quantity. Naively speaking, a quantum memory should be able to restore a signal in the tiniest details, beyond the quantum limit.

Resonant excitation of an atomic transition provides appropriate strong coupling between light and matter. However, interaction with a single atom is not enough to trap the incident photon with absolute certainty. One can increase the coupling by placing the atom inside a high finesse cavity. Instead, in the present course, we only consider trapping of light by a macrocopic ensemble of atoms.

We also need interrogate the memory at will, controlling the moment when the signal is restored. This can be achieved through an auxilliary optical transition, coupled to the quantum field capture transition. Several protocols rely on the Lambda three-level system. A common upper level links the two transitions that are connected to two sub-levels of the electronic ground state.

The quantum-properties preserving storage of one photon is an unitary process. Initially, the single excitation light state is combined with the material medium ground state. The compound system undergoes an unitary transform towards a state where the unique excitation has been transposed to matter. The stored information is retrieved with the help of the reverse unitary transform. What makes the process so difficult is precisely the unitary transform that involves a macroscopic ensemble of atoms. One can certainly convert one photon into an excitation of a strongly absorbing medium. This

is not enough to make a quantum memory. A single photon pulse is characterized by a spatial mode and a spectro-temporal distribution. Generally an incident photon only transfers its energy to the absorbing medium. The photon will be reemitted eventually, after multiple reabsorption and scattering, in a spatial and spectro-temporal state devoid of any connection with the initial state.

The reason why energy alone is transferred to the medium is not so obvious. When exposed to optical excitation, a two-state atom, initially in the ground level, is promoted to a quantum superposition state. Quantum information thus flows from light to the atom. Provided that atoms are numerous enough one thus expects that all the incident light could be converted into quantum atomic excitation. However one is faced with several issues. First, in general, the medium does not return to initial state after readout, a condition to be fulfilled for total recovery of the quantum state of light. The recovered field, propagating along the same wavevector as the initial signal, grows from zero in the input side. Therefore the atoms close to the input side of the absorbing medium are the most strongly excited by the incoming light signal, but also undergo the smallest feedback from the restored field that fails to take them back to the ground state. The atomic state and retrieved field mismatch results in partial absorption and incomplete extraction of the stored information. In addition to this propagation issue, one should mention random redistribution of light by spontaneous emission and quantum state destruction by coherence relaxation. However, in many systems coherence lifetime remains compatible with the demonstration of quantum storage for light.

In this series of lectures we shall essentially examine two ways of efficiently restoring the signal field, that is to say two ways of addressing the propagation problem. One approach is known as Electromagnetically Induced Transparency. This is a radical way to deal with absorption. The storage medium is made transparent to the incoming signal, operating as a trap that closes once the quantum field is inside. The other approach takes advantage of rephasing procedures to optimize the signal reconstruction. We shall essentially restrict the discussion to semiclassical theory, assuming that, within the limits of linear conditions, an efficient recovery procedure generally applies to a quantum field if it works with a classical field.

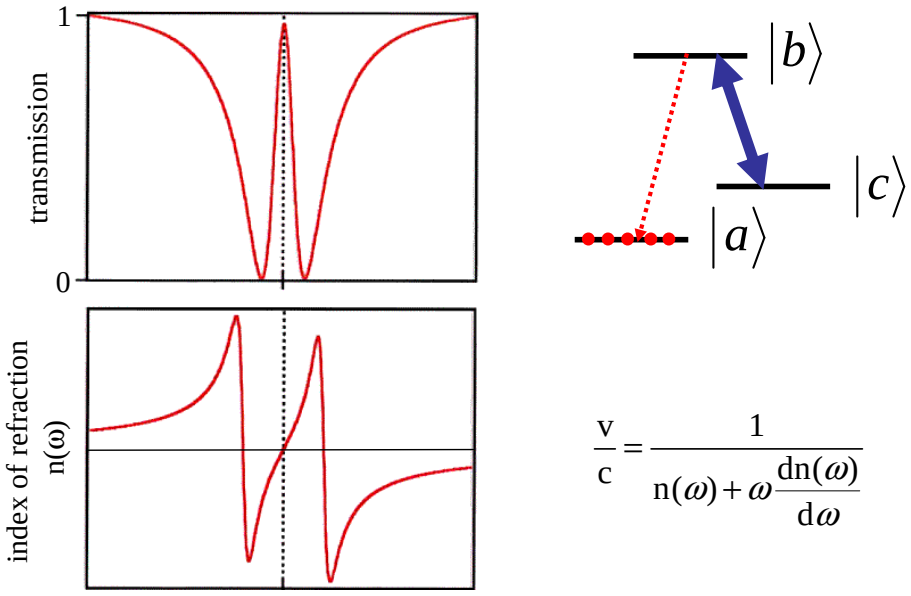

Figure 1: Principle of EIT. All atoms are initially prepared in state $|a\rangle$. The coupling field, resonant with the $b \rightarrow c$ empty transition, opens a transparency window on the $a \rightarrow b$ transition. The absorption profile distortion goes along with modified dispersion of the index of refraction. This is reflected in group velocity reduction within the transparency window.

2 Two ways of recovering light

2.1 Electromagnetically induced transparency and stopped light

As noticed above, the reconstructed signal tends to be reabsorbed during propagation through the storage medium. This problem is addressed in a radical way by Electromagnetically Induced Transparency (EIT), since the medium is made transparent at the signal input and output [2, 3]. With the help of an external control, the material opacity is switched on and off at will.

To control the opacity one resorts to an auxilliary optical transition that shares an atomic level with the storage transition. Hence, instead of two-level atoms, we have to consider an ensemble of three-level Λ-systems. Initially

all the atoms are in $|a\rangle$, which makes the medium absorbing on the $a \rightarrow b$ transition. Let us remind that absorption results from the coupling of the incident field with the reaction of the medium, represented by the macroscopic polarization density. EIT precisely proceeds through the annihilation of the polarization on the $a \rightarrow b$ transition. This is accomplished by a control field that resonantly excites the $b \rightarrow c$ auxilliary transition. When switched on, the control field converts the $a \rightarrow b$ optical polarization into the Raman coherence of states $|a\rangle$ and $|c\rangle$. The optical polarization vanishing renders the medium transparent on $a \rightarrow b$ (see Fig. 1). Since $b \rightarrow c$ connects empty levels, the medium is transparent on $b \rightarrow c$ too, so that all the atoms experience the same control field strength, wherever they are located in the absorbing medium.

The control field does not just open a transparency window. In accordance with Kramers Krönig relations, the distorsion of absorption profile is associated with a disturbance of the index of refraction, which results in the reduction of the group velocity v. In terms of dispersion of the refraction index $n(\omega)$, the group velocity v can be expressed as:

$$\frac{v}{c} = \frac{1}{\mathrm{n}(\omega) + \omega \dfrac{\mathrm{dn}(\omega)}{\mathrm{d}\omega}} \tag{1}$$

The field amplitude is continuous at the vacuum-medium interface. However the spatial extension of a signal pulse is compressed along the direction of propagation because of the velocity group reduction. The field envelope undergoes a v/c shrinking. The energy carried by the pulse is reduced by the same ratio, dropping close to zero when $v << c$. Actually energy transfer from the signal pulse to the control field comes along with the optical polarization conversion into Raman coherence. It is rather intriguing that the signal energy is taken away by the control field, while the spatial and spectro-temporal signal properties keep stored in the medium. Reverse transformation takes place at the active medium exit. The signal field then recovers its initial energy together with its spatial and spectro-temporal properties.

The EIT process has been demonstrated with classical light in various materials ranging from gas to condensed matter. Light speed reduction to 17 metres per second was observed in an ultracold atomic gas [4]. Then it was realized that light could not only be slowed down but even "stopped" in a Λ-system. Indeed, if the control field is switched off while the signal pulse is entirely contained within the active medium, the remaining properties

carried by the signal field are absorbed and lost, but most of them have been saved in the Raman coherence. If the control field is restored before the Raman coherence relaxes, the signal field is rebuilt, resumes its progression through the medium and finally exits, having preserved most of its initial characteristics [5, 6].

In the next sections we analytically derive the various operating conditions of the memory. Right now we can list most of them. We already noticed that information transfer to the Raman coherence is subject to the condition $v << c$. In order to be entirely contained within the L-thick material at the moment of the control field switching off, the signal pulse must exhibit a duration T smaller than L/v. Besides the signal bandwidth Δ must be smaller than the width of the transparency window. Finally those conditions must be consistent with the time and frequency Fourier conjugation, according to which $\Delta T > 1$.

It should be stressed that the control field, interacting with a transition between empty levels, does not excite any atoms on its own. As a consequence this field does not generate any noise. The signal field alone conveys excitation to the atomic ensemble.

Finally it should be noticed that EIT configuration imposes that the weak signal field should be isolated from the intense control field. This could be a major drawback.

2.2 Recovery from an absorbing medium

Instead of resorting to the radical solution of inducing transparency, one can try to retrieve the signal despite of medium absorption. We already noticed that the recovered field shall be weaker at the input side of the medium, precisely in the region where the incoming field is stronger. As a consequence the recovered field is unable to turn the atoms back into their initial state, which hampers correct information retrieval. In order to evade this obstacle, one can try to make the restored field to propagate in the opposite direction of the incoming signal field. This way, building up from the output side, the restored field gains strength all along the storage medium and is expected to reach its maximum intensity at the input side and to be intense enough there to turn the atoms back to the ground state.

Back scattering of the signal field reminds of phase conjugation in nonlinear optics. Three beams may be appropriate to reverse the direction of propagation. Again this can be combined with a three-level Λ-system. The

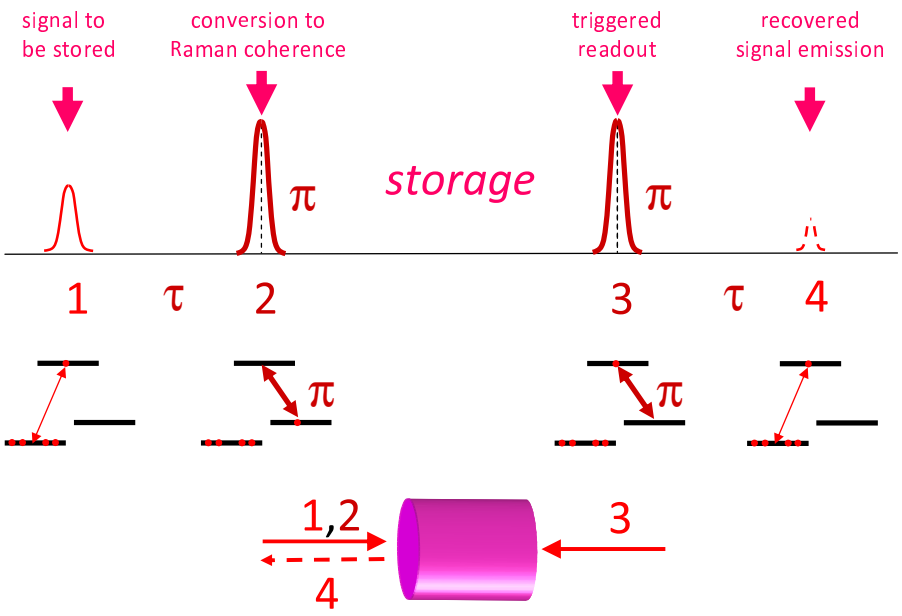

Figure 2: Signal recovery with reversed direction of propagation. Counterpropagating π-pulses are used to convert optical excitation into Raman coherence, then back to optical excitation. Therefore the restored signal propagates backward with respect to the incoming one.

signal to be stored propagating along $\vec{k}_1$ excites the $a \rightarrow b$ transition. Then a light pulse propagating along $\vec{k}_2$, resonant with the $b \rightarrow c$ transition, converts the optical excitation of $a \rightarrow b$ into the Raman coherence of states $|a\rangle$ and $|c\rangle$. A π-pulse can efficiently achieve such a conversion. The notion of pulse area will be defined later. Information is stored in the Raman coherence until another π-pulse, propagating along $\vec{k}_3$ converts back the Raman coherence into optical excitation of $a \rightarrow b$. In accordance with general phase matching conditions, the signal can be reconstructed in the direction $\vec{k}_3 + \vec{k}_2 - \vec{k}_1$, that is to say in direction $-\vec{k}_1$ provided $\vec{k}_3 = -\vec{k}_2$ (see Fig. 2).

If atoms are initially prepared in state $|a\rangle$, the medium is transparent to the conversion pulses. In addition, those pulses do not induce any excitation noise since the incoming signal field alone can convey excitation to the atomic ensemble.

Unfortunately it does not work so easily. The process relies on the time separation of the different steps, namely the capture of the incoming signal, the conversion to Raman coherence, the back conversion to optical excitation and the recovered signal emission. In order to be stored, the data pulse must be shorter than the $|a\rangle$ and $|b\rangle$ superposition state lifetime. Equivalently, the data pulse bandwidth must exceed the homogeneous linewidth. Yet, in an homogeneously broadened medium, where all atoms have the same transition frequency, the storage bandwidth is precisely limited by the homogeneous width, given by the inverse duration of the superposition state. Therefore one is faced with contradictory constraints, since the incoming pulse must simultaneously be narrower than the absorption profile, in order to be captured, and shorter than the superposition state lifetime, in order to be stored. In an effort to overcome the contradiction, let us consider an inhomogeneously broadened medium, where atoms exhibit different transition frequencies. The memory bandwidth is no longer limited by the inverse superposition state lifetime and much shorter signal pulses can be considered. Then one meets another obstacle. The superposition states that are built in different atoms evolve at different rates, which entails relative phase shift. The above described pulse sequence is unable to rephase the atoms, a necessary condition for signal recovery. We shall see how to solve this problem.

After the general presentation of the two memory architectures to be considered, we now proceed to the detailed analysis of the underlying physics.

3 Semi-classical description of light-matter interaction

3.1 Atom excitation by light

The sample is illuminated by travelling plane waves. The electromagnetic field is regarded as a classical quantity. The complex amplitude of the electric field is given by:

$$E(\vec{r},t) = \frac{1}{2}(\mathcal{E}(\vec{r},t) + \mathcal{E}^*(\vec{r},t)) = \frac{1}{2}(\mathcal{A}(\vec{r},t)\mathrm{e}^{i\omega_L t - i\vec{k}.\vec{r}} + c.c.) \tag{2}$$

The main time and space variation is collected in the phase factor $\mathrm{e}^{i\omega_L t - i\vec{k}.\vec{r}}$ that characterizes a wave with central frequency ω_L, propagating along a wave vector $\vec{k}$. The envelope $\mathcal{A}(\vec{r},t)$ little varies on the time and space scales of optical period and wavelength. The wave vector length is defined as $\omega_L = kc$.

The terms $\mathcal{E}(\vec{r},t)$ and $\mathcal{E}^*(\vec{r},t)$ respectively stand for the positive and negative frequency components of the field. Indeed the time-to-frequency Fourier transform of $\mathcal{E}(\vec{r},t)$, $\mathcal{E}(\vec{r},\omega) = \mathrm{F}[\mathcal{E}(\vec{r},t)]$, centered at optical frequency ω_L, is close to 0 at $-\omega_L$.

Interaction to the atomic system is described in electric dipole approximation by the hamiltonian:

$$H_I = -q\vec{R}.\vec{E} \tag{3}$$

where q is the (negative) electron charge. Thus $q = -e$, where e represents the elementary charge. The transition dipole matrix element between states $|i\rangle$ and $|j\rangle$:

$$\vec{\mu}_{ij} = \langle i|e\vec{R}|j\rangle \tag{4}$$

is defined with appropriate phase choice so that this element is real.

The atom density matrix equation reads as:

$$\begin{cases} \mathrm{i}\hbar\dot{\rho} &= [H,\rho] + \left.\dfrac{d\rho}{dt}\right|_{\text{relaxation}} \\ H &= H_0 - q\vec{R}\cdot\vec{E} = H_0 + e\vec{R}\cdot\vec{E} \end{cases} \tag{5}$$

This equation combines the unitary evolution, driven by the electromagnetic field, and the non-unitary evolution caused by coupling with environment. The latter is described by the phenomenological relaxation term.

In order to be more specific, let us first consider the interaction of a two-level atom with the incoming field. Expanding the density matrix equation on the set of eigenstates $|a\rangle, |b\rangle$ one obtains:

$$\left\{ \begin{array}{ll} \dot{\rho}_{aa} & = \mathrm{i}(\rho_{ab} - \rho_{ba})(\Omega \mathrm{e}^{\mathrm{i}\omega_L t - \mathrm{i}\vec{k}.\vec{r}} + \mathrm{c.c.}) + \gamma_b \rho_{bb} \\ \dot{\rho}_{bb} & = -\dot{\rho}_{aa} \\ \dot{\rho}_{ab} & = \mathrm{i}(\rho_{aa} - \rho_{bb})(\Omega \mathrm{e}^{\mathrm{i}\omega_L t - \mathrm{i}\vec{k}.\vec{r}} + \mathrm{c.c.}) + (\mathrm{i}\omega_{ab} - \gamma_{ab})\rho_{ab} \end{array} \right. \tag{6}$$

where the Rabi frequency is defined as:

$$\Omega(\vec{r}, t) = \frac{\mu_{ab} \mathcal{A}(\vec{r}, t)}{2\hbar} \tag{7}$$

If $\mathcal{A}(\vec{r}, t)$ is complex, the Rabi frequency is complex too. In order to separate the fast oscillation at optical frequency, one substitutes ρ_{ab} with:

$$\rho_{ab} = \tilde{\rho}_{ab} \mathrm{e}^{i\omega_L t - i\vec{k}.\vec{r}} \tag{8}$$

This is not a switch to interaction picture. In interaction representation one defines the operator $\rho_I = \exp(-\frac{i}{\hbar} H_0 t) \rho \exp(\frac{i}{\hbar} H_0 t)$ that involves a factor $\exp(-i\omega_{ab} t)$, specific to each frequency class. Instead, switching to the frame "rotating" at laser frequency, one applies the same tranform to all frequency classes. This difference will prove important in inhomogeneously broadened media where atoms oscillate at various frequencies.

Then, neglecting all the terms oscillating at harmonic overtones of ω_L, one obtains the *Rotating Wave Approximation* of the density matrix equation:

$$\left\{ \begin{array}{ll} \dot{\rho}_{aa} & = i(\tilde{\rho}_{ab}\Omega^* - \tilde{\rho}_{ba}\Omega) + \gamma_b \rho_{bb} \\ \dot{\rho}_{bb} & = -\dot{\rho}_{aa} \\ \dot{\tilde{\rho}}_{ab} & = i(\rho_{aa} - \rho_{bb})\Omega + (i\Delta - \gamma_{ab})\tilde{\rho}_{ab} \end{array} \right. \tag{9}$$

where $\Delta = \omega_{ab} - \omega_L$. One may formally integrate these equations. One first integrates the homogeneous equations. Then one takes the non-homogeneous term into account by the method of variation of the parameters. One obtains:

$$\left\{ \begin{array}{ll} n_{ab}(t) & = 1 + (n_{ab}(t_0) - 1)\mathrm{e}^{-\gamma_b(t-t_0)} + 2i \displaystyle\int_{t_0}^{t} dt' (\tilde{\rho}_{ab}\Omega^* - \tilde{\rho}_{ba}\Omega)\mathrm{e}^{-\gamma_b(t-t')} \\ \tilde{\rho}_{ab}(t) & = \tilde{\rho}_{ab}(t_0)\mathrm{e}^{(i\Delta - \gamma_{ab})(t-t_0)} + i \displaystyle\int_{t_0}^{t} dt' \Omega n_{ab} \mathrm{e}^{(i\Delta - \gamma_{ab})(t-t')} \end{array} \right. \tag{10}$$

Whether in differential or integral forms, these equations are known as optical Bloch equations. They rely on the following assumptions:

- interaction with the classical field is described in electric dipole approximation
- transition frequencies are constant parameters
- relaxation processes are described by phenomenological decay rates

The density matrix of a two-level atom is comprised of 4 components, 2 of which are complex. The trace conservation and the symmetry property $\rho_{ab} = \rho_{ba}^*$ reduce the number of independent parameters to 3, namely the population difference and the real and imaginary components of the coherence. Bloch equations are nothing but the three linear differential equations that couple these three quantities.

3.2 Radiative response

When prepared in a superposition of two states linked by an optical transition, the atoms behave as oscillating dipoles, i.e. as radiating microscopic antennas. They behave as real sources of Huyghens wavelets (see Fig. 3). In the same way as the virtual sources of Huyghens wavelets, the atoms acquire the space and time phase of the incoming field. As long as phase properties are preserved, that is to say as long as the atomic coherence has not been erased by homogeneous relaxation or phase-shift by inhomogeneous detuning, the atoms radiate as the virtual sources of Huyghens diffraction theory. Specifically, the spatial coherence of the sources makes the wavelets constructively interfere in the direction of the incoming wave. Elaborating the analysis a little further, one can determine the diffraction limited angular aperture of the emitted signal.

With this picture in mind, let us proceed to the local description of the atomic response, as derived from Maxwell equations. In a dielectric medium, in the absence of electric charges those equations read as:

$$\begin{aligned} \mathrm{rot}(\vec{E}) &= -\partial_t \vec{B} && \text{Faraday law} \\ \mathrm{rot}(\vec{B}) &= \partial_t \vec{D} && \text{Ampère theorem} \\ \mathrm{div}(\vec{D}) &= 0 && \text{Gauss theorem} \end{aligned} \tag{11}$$

where $\vec{D}$ can be expressed in terms of the macroscopic polarization density $\vec{P}$ as:

$$\vec{D} = \epsilon_0 \vec{E} + \vec{P} \tag{12}$$

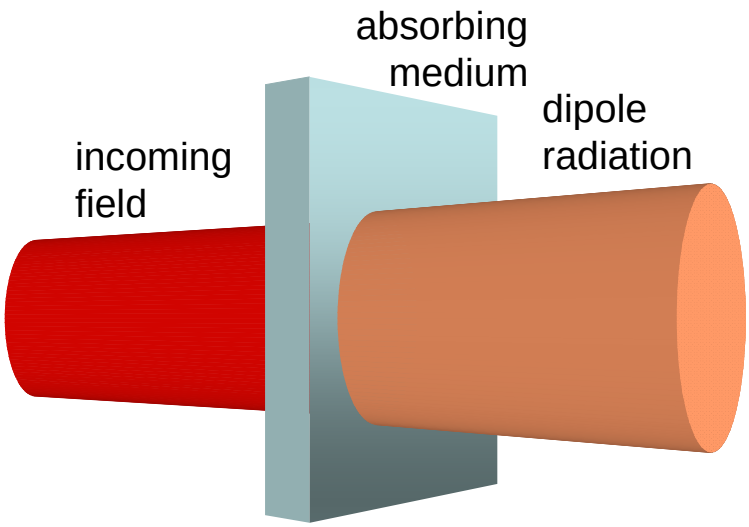

Figure 3: The coherent atomic response to optical excitation can be understood within the frame of Huyghens diffraction theory. The atomic dipoles behave as real sources of Huyghens wavelets.

These equations combine into the wave equation with sources:

$$\Delta\vec{E} - \mu_0\epsilon_0\frac{\partial^2\vec{E}}{\partial t^2} = \mu_0\frac{\partial^2\vec{P}}{\partial t^2} - \frac{1}{\epsilon_0}\text{grad}[\text{div}(\vec{P})] \tag{13}$$

The atomic response is contained in the macroscopic polarization density $\vec{P}$. We assume that the transverse variation of $\vec{P}$ is very small on the scale of the atomic wavelength. This enables us to drop the second term on the right hand side of Eq.13.

We have now to express the macroscopic polarization density in terms of the optical Bloch equation solutions. Let us consider the N atoms sitting within an elementary volume V. The size of this volume is small enough with respect to the optical wave length so that all the atoms interact with the same field. The total dipole moment is expressed as the sum of the N individual dipoles. The expectation value of the corresponding quantum observable reads as:

$$\left\langle \sum_{i=1}^{N}\mu_i \right\rangle = \text{Tr}\left[\left(\sum_{i=1}^{N}\mu_i\right)\boldsymbol{\rho}\right] \tag{14}$$

where $\boldsymbol{\rho}$ represents N-atom density operator. The N-atom state is initially factorizable and is assumed to remain so under semi-classical excitation. In other words, semi-classical excitation is expected not to entangle the N atoms. The density operator then reads as:

$$\boldsymbol{\rho} = \rho_1 \otimes \ldots \otimes \rho_i \otimes \ldots \otimes \rho_N \tag{15}$$

In order to express the total dipole in terms of the individual density matrices, one uses the relation:

$$\underset{1\cdots N\neq i}{\mathrm{Tr}}(\rho_1 \otimes \ldots \otimes \rho_i \otimes \ldots \otimes \rho_N) = \rho_i \tag{16}$$

Then the total dipole expectation value reduces to:

$$\left\langle \sum_{i=1}^{N} \mu_i \right\rangle = \sum_{i=1}^{N} \underset{i}{\mathrm{Tr}} \left[\underset{1\cdots N\neq i}{\mathrm{Tr}} (\mu_i \boldsymbol{\rho}) \right] = \sum_{i=1}^{N} \underset{i}{\mathrm{Tr}} \left(\mu_i \underset{1\cdots N\neq i}{\mathrm{Tr}} \boldsymbol{\rho} \right) = \sum_{i=1}^{N} \mathrm{Tr}(\mu_i \rho_i) \tag{17}$$

For the time being we ignore inhomogeneous broadening. All the atoms have the same transition frequency. Then the elementary volume dipole moment reads as:

$$\sum_{i=1}^{N} \mathrm{Tr}(\mu_i \rho_i) = -N\mu_{ab} \left[\rho_{ab}(\vec{r}, t) + \rho_{ba}(\vec{r}, t) \right] \tag{18}$$

where the sum runs over all the atoms within the elementary volume, with $\langle a|\mu|a\rangle = \langle b|\mu|b\rangle = 0$. A minus sign appears because μ_{ab} has been defined from the elementary charge e and not from the electron charge $q = -e$. Dividing by the volume V, one finally gets the macroscopic polarization density:

$$P(\vec{r}, t) = -n\mu_{ab} \left[\rho_{ab}(\vec{r}, t) + \rho_{ba}(\vec{r}, t) \right] \tag{19}$$

where n denotes the density of active atoms per unit volume.

In the same way as the electric field, the polarization density appears to be comprised of positive and negative frequency components. Those components do not overlap spectrally, being distant by hundreds of THz, so they satisfy uncoupled wave equations. The positive frequency component wave equation reads as:

$$\frac{1}{2} \left(\Delta - \frac{1}{c^2} \frac{\partial^2}{\partial t^2} \right) \left(\mathcal{A}(\vec{r}, t) \mathrm{e}^{\mathrm{i}\omega_L t - \mathrm{i}\vec{k}.\vec{r}} \right) = -n \frac{\mu_{ab}}{c^2 \epsilon_0} \frac{\partial^2}{\partial t^2} \left(\tilde{\rho}_{ab}(\vec{r}, t) \mathrm{e}^{\mathrm{i}\omega_L t - \mathrm{i}\vec{k}.\vec{r}} \right) \tag{20}$$

Within the frame of the *slowly varying envelope approximation*, we can neglect the contributions of order $\partial_t \mathcal{A}(\vec{r},t)/[\omega_L \mathcal{A}(\vec{r},t)]$ and $\nabla \mathcal{A}(\vec{r},t)/[k\mathcal{A}(\vec{r},t)]$. The wave equation then reduces to:

$$\left(\frac{\partial}{\partial z}+\frac{1}{c}\frac{\partial}{\partial t}\right)\mathcal{A}(\vec{r},t)=\mathrm{i}nk\frac{\mu_{ab}}{\epsilon_0}\tilde{\rho}_{ab}(\vec{r},t) \tag{21}$$

Substituting $\mathcal{A}(\vec{r},t)$ with Eq.7 one obtains:

$$\left(\frac{\partial}{\partial z}+\frac{1}{c}\frac{\partial}{\partial t}\right)\Omega(\vec{r},t)=\mathrm{i}nk\frac{\mu_{ab}^2}{2\hbar\epsilon_0}\tilde{\rho}_{ab}(\vec{r},t) \tag{22}$$

It is worth expressing this equation of propagation in terms of the resonant absorption coefficient α_0. To first order in $\Omega(\vec{r},t)$ the Bloch equation for $\tilde{\rho}_{ab}(\vec{r},t)$ reads as:

$$\tilde{\rho}_{ab}(\vec{r},t)=\mathrm{i}\int_{-\infty}^{t}\Omega(\vec{r},t')\mathrm{e}^{-\gamma_{ab}(t-t')}dt' \tag{23}$$

which reduces to $\tilde{\rho}_{ab}(\vec{r},t)=\mathrm{i}\Omega(\vec{r},t')/\gamma_{ab}$ if $\Omega(\vec{r},t)$ little varies on γ_{ab}^{-1} time scale. This condition simply means that the field bandwidth is much narrower than the absorption line, so that the polarization density instantaneously adjusts to the field variations. Substituting the expression of $\tilde{\rho}_{ab}(\vec{r},t)$ in Eq.22 one obtains:

$$\left(\frac{\partial}{\partial z}+\frac{1}{c}\frac{\partial}{\partial t}\right)\Omega(\vec{r},t)=-nk\frac{\mu_{ab}^2}{2\hbar\epsilon_0\gamma_{ab}}\Omega(\vec{r},t)=-\frac{\alpha_0}{2}\Omega(\vec{r},t) \tag{24}$$

Finally the wave equation reads as:

$$\left(\frac{\partial}{\partial z}+\frac{1}{c}\frac{\partial}{\partial t}\right)\Omega(\vec{r},t)=\mathrm{i}\frac{\alpha_0\gamma_{ab}}{2}\tilde{\rho}_{ab}(\vec{r},t) \tag{25}$$

4 Three-level Λ-system, EIT

4.1 Optical excitation of the Λ-system

In a Λ-system an upper state $|b\rangle$ is connected through optical transitions to two lower states $|a\rangle$ and $|c\rangle$. The system is illuminated by two driving fields. The $a \rightarrow b$ and $b \rightarrow c$ transitions are respectively driven at frequencies ω_1

and ω_2 with Rabi frequencies Ω_1 and Ω_2. Each driving field is assumed to excite a single transition. Angular selection rules may help to discriminate the transitions. Indeed cross-polarizing the light beams may be enough to separately drive the two transitions when such selection rules apply. Otherwise, the splitting ω_{ac} must be much larger than the homogeneous widths, the Rabi frequencies and the detunings $|\omega_{ab}-\omega_1|$ and $|\omega_{bc}-\omega_2|$. The adjunction of a third state significantly complicates the density matrix formalism. Instead of 3 real independent parameters in a two-level system, one is left with 8 real parameters in a three-level atom. Those quantities are coupled by the following differential linear equations:

$$\left\{\begin{array}{ll}
\dot{\rho}_{aa} & = \mathrm{i}(\tilde{\rho}_{ab}\Omega_1^* - \tilde{\rho}_{ba}\Omega_1) + r_a\gamma_b\rho_{bb} \\
\dot{\rho}_{cc} & = \mathrm{i}(\tilde{\rho}_{cb}\Omega_2^* - \tilde{\rho}_{bc}\Omega_2) + r_c\gamma_b\rho_{bb} \\
\dot{\rho}_{bb} & = -\dot{\rho}_{aa} - \dot{\rho}_{cc} \\
\dot{\tilde{\rho}}_{ab} & = [\mathrm{i}(\omega_{ab}-\omega_1) - \gamma_{ab}]\tilde{\rho}_{ab} + \mathrm{i}(\rho_{aa}-\rho_{bb})\Omega_1 + \mathrm{i}\tilde{\rho}_{ac}\Omega_2 \\
\dot{\tilde{\rho}}_{cb} & = [\mathrm{i}(\omega_{bc}-\omega_2) - \gamma_{bc}]\tilde{\rho}_{cb} + \mathrm{i}(\rho_{cc}-\rho_{bb})\Omega_2 + \mathrm{i}\tilde{\rho}_{ca}\Omega_1 \\
\dot{\tilde{\rho}}_{ac} & = [\mathrm{i}(\omega_{ac}-\omega_1+\omega_2) - \gamma_{ac}]\tilde{\rho}_{ac} + \mathrm{i}(\tilde{\rho}_{ab}\Omega_2^* - \tilde{\rho}_{bc}\Omega_1)
\end{array}\right. \tag{26}$$

The system is assumed to be closed. The coefficients r_a and $r_c = 1 - r_a$ account for the upper level relaxation distribution between the two ground sublevels. As usual in the rotating wave picture, the off-diagonal matrix elements have been substituted with:

$$\begin{array}{ll}
\rho_{ab} & = \tilde{\rho}_{ab}\mathrm{e}^{\mathrm{i}\omega_1 t - \mathrm{i}\vec{k_1}.\vec{r}} \\
\rho_{cb} & = \tilde{\rho}_{cb}\mathrm{e}^{\mathrm{i}\omega_2 t - \mathrm{i}\vec{k_2}.\vec{r}} \\
\rho_{ac} & = \tilde{\rho}_{ac}\mathrm{e}^{\mathrm{i}(\omega_1-\omega_2)t - \mathrm{i}(\vec{k_1}-\vec{k_2}).\vec{r}}
\end{array} \tag{27}$$

The first three lines of Eq.26 express the population evolution. This does not differ from the corresponding two-level system equations. The last three lines of Eq.26, accounting for coherence evolution, are more specific. First one observes that coherence ρ_{ac} is excited by the light fields, although no direct transition connects states $|a\rangle$ and $|c\rangle$. Besides, coherences ρ_{ab} and ρ_{bc} are coupled not only to level populations, but also to ρ_{ac}. For instance, coherence ρ_{ab} is built not only from direct excitation of state $|a\rangle$ population by field Ω_1, but also from the excitation of coherence ρ_{ac} by field Ω_2.

The system evolution is generally complex when both fields are applied simultaneously. One observes phenomena such as stimulated Raman adiabatic passage (STIRAP) [7], dark resonance [8], or the EIT process we are about to examine more carefully.

However, the excitation of ρ_{ac}, also known as the Raman coherence, gives rise to attractive features even when the fields Ω_1 and Ω_2 do not interact simultaneously with the system. We shall meet such features within the frame of signal reconstruction in an absorbing medium.

4.2 Solving the Bloch equations with EIT conditions

In this section we follow the lines of Ref. [9]. With the following assumptions:

- all the atoms are initially prepared in state $|a\rangle$
- Ω_2, known as the "coupling" or "control" field, is a constant.
- Ω_1, carrying the information to be stored, has a pulse area $<< 1$

the density matrix equations get much simpler. To first order in Ω_1, the level population does not vary and the term $\tilde{\rho}_{bc}\Omega_1$ can be neglected. Therefore the equations of ρ_{ab} and ρ_{ac} turn into:

$$\begin{aligned} \dot{\tilde{\rho}}_{ab} &= [\mathrm{i}(\omega_{ab} - \omega_1) - \gamma_{ab}]\tilde{\rho}_{ab} + \mathrm{i}\Omega_1 + \mathrm{i}\tilde{\rho}_{ac}\Omega_2 \\ \dot{\tilde{\rho}}_{ac} &= [\mathrm{i}(\omega_{ac} - \omega_1 + \omega_2) - \gamma_{ac}]\tilde{\rho}_{ac} + \mathrm{i}\tilde{\rho}_{ab}\Omega_2^* \end{aligned} \tag{28}$$

In addition we assume the coupling field resonantly excites the $b \rightarrow c$ transition, and the signal pulse central frequency ω_1 coincides with ω_{ab}. The equations reduce to:

$$\dot{\tilde{\rho}}_{ab} = -\gamma_{ab}\tilde{\rho}_{ab} + \mathrm{i}(\Omega_1 + \tilde{\rho}_{ac}\Omega_2) \tag{29}$$

$$\dot{\tilde{\rho}}_{ac} = -\gamma_{ac}\tilde{\rho}_{ac} + \mathrm{i}\tilde{\rho}_{ab}\Omega_2^* \tag{30}$$

Substituting Eq. 30 into Eq. 29, one obtains:

$$\tilde{\rho}_{ac} = -\frac{\Omega_1}{\Omega_2} - \frac{\mathrm{i}}{\Omega_2}(\partial_t + \gamma_{ab})\tilde{\rho}_{ab} = -\frac{\Omega_1}{\Omega_2} - \frac{1}{|\Omega_2|^2}(\partial_t + \gamma_{ab})(\partial_t + \gamma_{ac})\tilde{\rho}_{ac} \tag{31}$$

If $\tilde{\rho}_{ac}$ reduces to the first term on the right hand side of Eq. 31, then the driving term $\Omega_1 + \tilde{\rho}_{ac}\Omega_2$ vanishes in Eq. 29. In other words, the Raman coherence contribution interferes with single-photon excitation to prevent the buildup of ρ_{ab}. The absence of atomic response to Ω_1 on the $a \rightarrow b$ transition is reflected by the absence of Ω_1 absorption.

This occurs if the second term on the right hand side of Eq.31 can be neglected, i.e. if:

$$(\partial_t + \gamma_{ab})(\partial_t + \gamma_{ac})\Omega_1 << \Omega_1/|\Omega_2|^2 \tag{32}$$

Then $\tilde{\rho}_{ac}$ adiabatically follows the variations of Ω_1. Given that $\rho_{aa} \cong 1$, the solution $\tilde{\rho}_{ac} = -\Omega_1/\Omega_2$ actually corresponds to the dark state:

$$|D\rangle = \frac{\Omega_2}{\sqrt{\Omega_1^2 + \Omega_2^2}}|a\rangle - \frac{\Omega_1}{\sqrt{\Omega_1^2 + \Omega_2^2}}|c\rangle \tag{33}$$

This is an important feature of EIT: interaction with the signal field Ω_1 immediately starts in the dark state, unlike what occurs in other three-level processes such as Coherent Population Trapping (CPT)[8].

Substituting $\tilde{\rho}_{ac}$ into Eq. 30, one finally obtains the expression of optical coherence:

$$\tilde{\rho}_{ab} = \frac{\mathrm{i}}{|\Omega_2|^2}(\partial_t + \gamma_{ac})\Omega_1, \tag{34}$$

from which we can calculate the atomic feedback on the incoming signal field Ω_1.

4.3 EIT wave equation

Substituting Eq. 34 into Eq. 25 one obtains:

$$\left[\frac{\partial}{\partial z} + \left(\frac{1}{c} + \frac{\alpha_0\gamma_{ab}}{2|\Omega_2|^2}\right)\frac{\partial}{\partial t}\right]\Omega_1(\vec{r},t) = -\frac{\alpha_0}{2}\frac{\gamma_{ab}\gamma_{ac}}{|\Omega_2|^2}\Omega_1(\vec{r},t) \tag{35}$$

This equation takes the usual form describing resonant plane wave propagation through an ensemble of two-level atoms in the linear regime. However, the propagation parameters are deeply altered:

- the absorption coefficient is reduced from α_0 to:

$$\alpha_\Omega = \alpha_0\frac{\gamma_{ab}\gamma_{ac}}{|\Omega_2|^2} \tag{36}$$

  With typical γ_{ab} and γ_{ac} values of about $10^6 s^{-1}$ and $10^3 s^{-1}$ respectively, an Ω_2 control field Rabi frequency of order 3 $10^5 s^{-1}$ is enough to reduce opacity by two orders of magnitude.

- the group velocity is reduced from c to:

$$v = \left(\frac{1}{c} + \frac{\alpha_0 \gamma_{ab}}{2|\Omega_2|^2} \right)^{-1} \tag{37}$$

  With the same numerical parameters, and with $\alpha_0 = 10^3 m^{-1}$, the group velocity amounts to no more than $200 m/s$!

The wave equation also tells us that, within the transparency window, an incoming travelling wave of the form $\Omega_1(t - z/c)$ in free space turns into the form $\Omega_1(t - z/v)$ as it propagates through the active medium. The wave preserves its temporal profile, just undergoing spatial compression by the factor v/c. The field amplitude is also preserved due to continuity at the interface of free space and active medium. Therefore neither the incoming signal duration nor its spectral width is affected by slowing down, provided that the signal is contained within the transparency window. Now we need clarify the notion of *transparency window*.

The EIT wave equation has been derived within the adiabatic condition limits. The incoming field variations have been assumed to be slow enough so that the Raman coherence can instantaneously adjust to them. One expects the adiabatic condition to fail if the incoming field varies too rapidly, i.e. if its spectral width exceeds some limiting value. Let us characterize the signal spectra width by the quantity $\Omega_1^{-1} \partial_t \Omega_1$. Let the signal be narrower than the absorption linewidth γ_{ab}, which leads to: $(\partial_t + \gamma_{ab})\Omega_1 \cong \gamma_{ab}\Omega_1$. Then the adiabatic condition reads as $(\partial_t \Omega_1)/\Omega_1 << |\Omega_2|^2/\gamma_{ab}$. The transparency width would thus be given by $\delta_T = |\Omega_2|^2/\gamma_{ab}$. This result need be examined more carefully. The differential equations we rely on − Bloch equation and wave equation − only convey local description, as illustrated by the linear absorption coefficient. However, we need the overall transmission through the entire atom ensemble to define the transparency window. Let the absorption coefficient at Δ from resonance be approximated by the function: $\alpha(\Delta) = \alpha_0[1 - \mathrm{e}^{-(\Delta/\delta_T)^2}]$. Then the transmission factor reads as $\mathrm{e}^{-\alpha(\Delta)L} \cong \mathrm{e}^{-\alpha_0 L(\Delta/\delta_T)^2}$, which finally leads to the transparency width:

$$\Delta_T = \delta_T / \sqrt{\alpha_0 L} = \frac{|\Omega_2|^2}{\gamma_{ab}\sqrt{\alpha_0 L}} \tag{38}$$

4.4 Storage and retrieval, stopped light

The energy carried by the incoming signal can be expressed as:

$$\int |\Omega_1(t - z/c)|^2 \, \mathrm{d}z = c \int |\Omega_1(t - x)|^2 \, \mathrm{d}x \tag{39}$$

If one is able to have the entire pulse standing within the active medium, the carried energy becomes, inside the material:

$$\int |\Omega_1(t - z/v)|^2 \, \mathrm{d}z = \frac{v}{c} \int |\Omega_1(t - z/c)|^2 \, \mathrm{d}z \tag{40}$$

which represents a v/c reduction with respect to the free space value. Therefore most of the energy has been extracted from the field if $v << c$. It can be shown that energy has been transferred to the control field, as soon as the signal field crosses the free space to material interface. Nonetheless, the Raman coherence is expressed as Ω_1/Ω_2, being proportional to the instantaneous signal field. Therefore, a spin wave propagates within the material along with the signal field, although the latter does not carry any energy.

If one abruptly switches off the control field, the residual signal field disappears, being absorbed by the material, while the spin wave stops propagating, but survives as long as permitted by decoherence processes. One improperly says that light is "stopped". Actually one should say that the signal field has been split into two parts. On the one hand, its energy has been removed by the control field. On the other hand its information content has been stored in the Raman coherence [10].

When the control field is turned back on, the signal field is rebuilt from the Raman coherence. The restored field resumes its progression, pulling its companion spin wave. Energy is fed back to the field at the output of the active medium.

To "stop" light without losing information, one has to make the entire signal pulse to stand within the boundaries of the active medium. The part of the signal entering the storage medium after control field shutdown is lost by absorption. The spatial extension of a pulse with duration τ is $v\tau$. This has to be smaller than the material thickness L. Besides the signal spectral width Δ must be smaller than the transparency width Δ_T. Combining those two conditions leads to:

$$\Delta \ \tau << \Delta_T L/v = \sqrt{\alpha_0 L} \tag{41}$$

With the additional condition $\Delta\ \tau > 1$, because of time-frequency Fourier conjugation, the "stopped" light storage requirement reads as:

$$\sqrt{\alpha_0 L} >> 1 \tag{42}$$

4.5 Limits of the semi-classical picture

In a "stopped" light process, a single photon trapping is expected to leave the atom ensemble in the following superposition state:

$$|\Psi_1\rangle = \frac{1}{\sqrt{N}} \left(\mathrm{e}^{\mathrm{i}\phi(\vec{r}_1)} |ca\cdots a\rangle + \mathrm{e}^{\mathrm{i}\phi(\vec{r}_2)} |ac\cdots a\rangle + \cdots + \mathrm{e}^{\mathrm{i}\phi(\vec{r}_N)} |aa\cdots c\rangle \right) \tag{43}$$

This is a collective single excitation state where the sum runs over all the atoms interacting with the field. All the atoms are considered on an equal footing, which does not perfectly account for the finite spatial extension of the stored light pulse. However this does not interfere with the general meaning of the present discussion.

The collective state appears to be entangled. It cannot be factorized as a product of individual atom states. This is precisely the type of state that cannot be produced in the frame of a semiclassical picture analysis. In the semiclassical approach the atoms communicate with outside world through a classical field that does not convey any quantum information. As a result, collective excitation, with all atoms considered on an equal footing, can only build ensemble product states such as the following:

$$(1+\epsilon^2)^{-N/2} \left(|a\rangle + \epsilon \mathrm{e}^{\mathrm{i}\phi(\vec{r}_1)} |c\rangle \right) \left(|a\rangle + \epsilon \mathrm{e}^{\mathrm{i}\phi(\vec{r}_2)} |c\rangle \right) \cdots \left(|a\rangle + \epsilon \mathrm{e}^{\mathrm{i}\phi(\vec{r}_N)} |c\rangle \right) \tag{44}$$

This state can be expanded as a sum of n-excitation states:

$$(1+\epsilon^2)^{-N/2} \left\{ |\Psi_0\rangle + \epsilon\sqrt{N}\, |\Psi_1\rangle + \epsilon^2 \sqrt{\frac{N(N-1)}{2!}}\, |\Psi_2\rangle + \cdots + \epsilon^N\, |\Psi_N\rangle \right\} \tag{45}$$

where $|\Psi_1\rangle$ is defined above and where:

$$\begin{array}{ll} |\Psi_0\rangle & = |aa\cdots a\rangle \\ |\Psi_2\rangle & = \sqrt{\frac{2!}{N(N-1)}} \left(\mathrm{e}^{\mathrm{i}(\phi(\vec{r}_1)+\phi(\vec{r}_2))} |cca\cdots a\rangle + \mathrm{e}^{\mathrm{i}(\phi(\vec{r}_1)+\phi(\vec{r}_3))} |cac\cdots a\rangle + \cdots \right) \\ \cdots & \cdots\cdots\cdots\cdots \\ |\Psi_N\rangle & = \mathrm{e}^{\mathrm{i}(\phi(\vec{r}_1)+\cdots+\phi(\vec{r}_N))}\, |cc\cdots c\rangle \end{array} \tag{46}$$

The 1-excitation component coincides with the previously defined single excitation entangled state $|\Psi_1\rangle$. In the n-excitation states expansion, the weight of $|\Psi_1\rangle$, as given by $\epsilon^2 N/(1+\epsilon^2)^{-N} \cong \epsilon^2 N \mathrm{e}^{-N\epsilon^2}$, never exceeds $1/e$, a value that is reached at $\epsilon^2 N = 1$ and equals the weight of the 0-excitation state $|\Psi_0\rangle$. Since ϵ^2 represents state $|c\rangle$ population in an individual atom, $\epsilon^2 N$ corresponds to the average number of atoms in $|c\rangle$. Therefore the weight of $|\Psi_1\rangle$ is maximum when the average number of atoms in $|c\rangle$ is unity. More generally, one easily checks that the n-excitation state distribution obeys Poisson statistics and is consistent with excitation by a coherent state of the field but is never consistent with excitation by a Fock state of the field, with a fixed number of photons.

4.6 Single photon storage and retrieval: experiment

The first observation of single photon storage and retrieval is published in December 2005 [11]. A laser-cooled atom cloud is used as the storage material. The cloud contains about 4 10^9 ^{85}Rb atoms, cooled to $100\mu K$ in a magneto-optic trap.

The quantum light signal has to be narrower than the Rubidium D1 line, a few MHz-wide. No parametric light source is able to generate such monochromatic single photons. A specific source has to be developed first. Another cloud, identical to the memory ensemble, plays this role. A strongly attenuated classical beam, directed along $\vec{k}_1$, illuminates this cloud (see Fig. 4. One waits for Raman scattering in direction $\vec{k}_2$. Detection of a Raman photon in this direction projects the atom cloud to the single excitation state:

$$\frac{1}{\sqrt{N}}\left(\mathrm{e}^{-\mathrm{i}(\vec{k}_1-\vec{k}_2).\vec{r}_1}|ca\cdots a\rangle + \mathrm{e}^{-\mathrm{i}(\vec{k}_1-\vec{k}_2).\vec{r}_2}|ac\cdots a\rangle + \cdots + \mathrm{e}^{-\mathrm{i}(\vec{k}_1-\vec{k}_2).\vec{r}_N}|aa\cdots c\rangle\right) \tag{47}$$

where a and c refer to the ground substates of the atoms, considered as three-level Λ-systems. As soon as a photon is detected on PD1, a rather intense pulse is directed to the source cloud along $-\vec{k}_1$. In synchrony with this pulse, a single photon is emitted in direction $-\vec{k}_2$, with probability close to unity. This emission corresponds to stimulated Raman scattering on the previously prepared single-excitation ensemble superposition state. The radiated single photon is then directed through an optical fiber to the memory cloud. The arrival time in the memory is known from the event detection on PD1. One switches off the control field in order to "stop" or to "trap" the photon

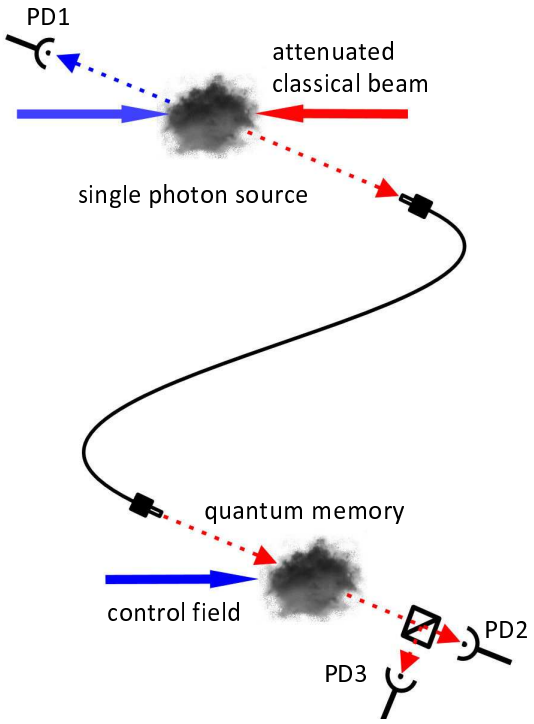

Figure 4: Single photon storage and retrieval [11]. The single photon source and the memory are both clouds of laser-cooled Rb atoms. PD1, 2, 3 represent photodetectors.

inside the memory. One turns back on this field to restore the photon. To check the unicity of the recovered photon, one performs an anti-correlation measurement on PD2 and PD3, following the Hanbury Brown and Twiss procedure. The memory lifetime appears to be no more than $10\mu s$. This is assigned to magnetic field inhomogeneity.

5 EIT in a solid: inhomogeneous broadening

5.1 Line broadening and relaxation

The most critical EIT parameter is the Raman coherence lifetime, but this does not restrict the choice of material to such sophisticated systems as LCAC. Long coherence lifetime can also be found in solid materials at liquid helium temperature. In such materials the absence of motion keeps the active centers from migrating outside the light beams, as in LCAC, but even better since motion is totally absent. One also avoids spatial dephasing that can affect superposition states and can be caused by diffusion, even in LCAC. Rare earth ion doped crystals have been considered as potential solid material candidates for quantum memory applications. Offering similar coherence lifetime properties as atomic samples, they differ from LCAC by the large inhomogeneous broadening of their spectral lines.

In LCAC the atoms move so slowly that the Doppler shift does not affect the absorption line profile. In solid materials the absence of motion of the absorbing centers reflects the strength of their interaction with the crystal. Interaction entails energy level shift and, because the crystal is never perfect, the shift varies from site to site. As a result the transition frequency is not unique for all the absorbing centers. Instead the transition frequency is distributed over a broad spectral interval, whose width W_{ab}, named the inhomogeneous width, typically ranges from a few GHz to several tens of GHz.

Before incorporating inhomogeneous broadening in EIT analysis, we need clarify different aspects of interaction with environment. On the one hand, the interaction shifts the energy levels, which results in the inhomogeneous broadening. This represents a static aspect. Cooling down to a few Kelvins does not significantly change the level shift. On the other hand, interaction also exhibits a dynamical aspect, corresponding to interaction fluctuations. On an $a \rightarrow b$ transition, this is reflected in the excess of the homogeneous

width γ_{ab} with respect to half the population decay rate $\gamma_b/2$. When the sample is cooled down, γ_{ab} decreases and gets closer to $\gamma_b/2$.

However homogeneous and inhomogeneous width are not different in essence. This is a question of observation time scale. Such effect that appears as a fluctuation at a given time scale, and thus contributes to homogeneous broadening, may be regarded as a static feature on a shorter time scale, and then pertain to inhomogeneous broadening.

In the absence of inhomogeneous broadening we have performed the analysis in the vicinity of single-photon resonance. This is not valid anymore in case of large inhomogeneous broadening. Spectral distance to single-photon resonance varies dramatically among the atoms. Instead of performing the analysis in time domain, we now consider a spectral domain approach, through time-to-frequency Fourier transform.

5.2 Polarization and susceptibility

To account for the distribution of transition frequencies, we rewrite the macrocopic polarization density in the form:

$$P(\vec{r},t) = -\mu_{ab} \int \mathrm{d}\omega_{ab} G(\omega_{ab}) \left[\rho_{ab}(\vec{r},t;\omega_{ab}) + \rho_{ba}(\vec{r},t;\omega_{ab})\right] \tag{48}$$

where $G(\omega_{ab})$ stands for the spectral and spatial distribution law, normalized to the atom density per unit volume n as: $\int \mathrm{d}\omega_{ab} G(\omega_{ab}) = n$. Time to frequency Fourier transform leads to:

$$\hat{P}(\vec{r},\omega) = -\mu_{ab} \int \mathrm{d}\omega_{ab} G(\omega_{ab}) \left[\hat{\rho}_{ab}(\vec{r},\omega;\omega_{ab}) + \hat{\rho}_{ba}(\vec{r},\omega;\omega_{ab})\right] \tag{49}$$

In linear optics conditions, which apply to our weak signal field, the polarization can be expressed as:

$$\hat{P}(\vec{r},\omega) = \epsilon_0 \chi(\omega) E(\vec{r},\omega) \tag{50}$$

where $\chi(\omega)$ denotes the electric susceptibility. This formula, well known in electrostatics, also applies to electrodynamics, *provided the relevant quantities are expressed in the frequency domain*[1]. Splitting the susceptibility

[1]If $\chi(\omega)$ varies slowly over the field spectral width, the following approximation:

$$P(\vec{r},t) = F\left[\hat{P}(\vec{r},\omega)\right] \cong \epsilon_0 \chi(\omega) F\left[E(\vec{r},\omega)\right] = \epsilon_0 \chi(\omega) E(\vec{r},t)$$

and the field amplitude into positive and negative frequency components one obtains:

$$\hat{P}(\vec{r},\omega) = \epsilon_0 \left[\chi^{(+)}(\omega) + \chi^{(-)}(\omega)\right] \frac{1}{2} \left[\hat{\mathcal{E}}(\vec{r},\omega) + \hat{\mathcal{E}}^*(\vec{r},-\omega)\right] \tag{51}$$

The positive (resp. negative) frequency component of the field vanishes in the $\omega \approx -\omega_1$ (resp. $\omega \approx \omega_1$) region. Likewise the positive (resp. negative) frequency component of the susceptibility vanishes in the $\omega \approx -\omega_{ab}$ (resp. $\omega \approx \omega_{ab}$) region. Therefore the cross-term $\chi^{(+)}(\omega)\hat{\mathcal{E}}^*(\vec{r},-\omega) + \chi^{(-)}(\omega)\hat{\mathcal{E}}(\vec{r},\omega)$ vanishes and the polarization density finally reads as:

$$\hat{P}(\vec{r},\omega) = \frac{1}{2}\epsilon_0 \left[\chi^{(+)}(\omega)\hat{\mathcal{E}}(\vec{r},\omega) + \chi^{(-)}(\omega)\hat{\mathcal{E}}^*(\vec{r},-\omega)\right] \tag{52}$$

In order to determine the susceptibility, let us come back to the three-level system Bloch equation. The transition frequency is now distributed over the inhomogeneous width of the absorption line. We still assume that:

- all atoms, whatever their transition frequency, initially sit in state $|a\rangle$
- the signal (resp. the control) field only excites the $a \to b$ (resp. $b \to c$) transition

As we already noticed, cross-polarizing the light beams may be enough to separately drive the two transitions when angular selection rules apply. However, when the two transitions only differ by their frequency, they are coupled to a single specific field only if the ground state splitting is much larger than the homogeneous widths, the Rabi frequencies and the transition detunings. This requires that $W_{ab} << \omega_{ac}$. We shall see how to cope practically with this condition.

Since Ω_2 is a constant, the Bloch equations for $\tilde{\rho}_{ab}$ and $\tilde{\rho}_{ac}$ are linear expressions of time dependent quantities and can be solved by Fourier transformation. In terms of ρ_{ab}, $\mathcal{E}(\vec{r},t)$ and the new variable $\zeta = \tilde{\rho}_{ac}\mathrm{e}^{\mathrm{i}(\omega_1 t - \vec{k}_1.\vec{r})}$,

makes the time dependent polarization density proportional to the field, as in the frequency domain. This implies instantaneous response to optical excitation and obscures the causal character of the material reaction. The general expression, fully accounting for causality, reads as:

$$P(\vec{r},t) = F\left[\hat{P}(\vec{r},\omega)\right] = \epsilon_0 \int \mathrm{d}\tau \check{\chi}(\tau) E(\vec{r},t-\tau)$$

where $\check{\chi}(\tau) = 0$ when $\tau \leq 0$

Eqs. 29 and 30 turn into:

$$\begin{aligned} \dot{\rho}_{ab} &= [\mathrm{i}\omega_{ab} - \gamma_{ab}]\rho_{ab} + \mathrm{i}\frac{\mu_{ab}\mathcal{E}(\vec{r},t)}{2\hbar} + \mathrm{i}\zeta\Omega_2 \\ \dot{\zeta} &= [\mathrm{i}(\omega_{ac}+\omega_2) - \gamma_{ac}]\zeta + \mathrm{i}\rho_{ab}\Omega_2^* \end{aligned} \tag{53}$$

Proceeding to Fourier transformation one gets:

$$\begin{aligned} [\mathrm{i}(\omega-\omega_{ab}) + \gamma_{ab}]\hat{\rho}_{ab}(\omega) &= \mathrm{i}\frac{\mu_{ab}\hat{\mathcal{E}}(\vec{r},\omega)}{2\hbar} + \mathrm{i}\hat{\zeta}(\omega)\Omega_2 \\ [\mathrm{i}(\omega-\omega_{ac}-\omega_2) + \gamma_{ac}]\hat{\zeta}(\omega) &= \mathrm{i}\hat{\rho}_{ab}(\omega)\Omega_2^* \end{aligned} \tag{54}$$

By eliminating $\hat{\zeta}(\omega)$ one finally obtains the optical coherence expression[2] :

$$\hat{\rho}_{ab}(\omega) = \mathrm{i}\frac{\mu_{ab}\hat{\mathcal{E}}(\vec{r},\omega)}{2\hbar}\frac{\mathrm{i}(\omega-\omega_{ac}-\omega_2)+\gamma_{ac}}{[\mathrm{i}(\omega-\omega_{ab})+\gamma_{ab}][\mathrm{i}(\omega-\omega_{ac}-\omega_2)+\gamma_{ac}]+|\Omega_2|^2} \tag{55}$$

This expression depends on both the $\omega-\omega_{ab}$ detuning of the $a\rightarrow b$ single-photon transition to the $\hat{\mathcal{E}}(\vec{r},\omega)$ signal field component, and the $\omega-\omega_{ac}-\omega_2$ detuning of the $a\rightarrow c$ two-photon transition to the compound excitation by $\hat{\mathcal{E}}(\vec{r},\omega)$ and the control field at ω_2. Let $\omega_{ab}^{(0)}$ represent the center of the atom spectral distribution $G(\omega_{ab})$. For sake of simplicity the splitting ω_{ac} is assumed to be the same in all the atoms. In other words, we suppose the $a\rightarrow c$ Raman transition is not inhomogeneously broadened. In general this is not true in a solid, but accounting for Raman frequency distribution proceeds along the same lines as the present calculation and can be extrapolated easily.

[2]The coherence $\rho_{ab}(t)$ must satisfy the causality condition. Thus $\rho_{ab}(t)$ does not depend on $\mathcal{E}(\vec{r},t')$, with $t'>t$. This condition can be translated to the frequency domain. By inverse Fourier transformation $\rho_{ab}(t)$ can be expressed as:

$$\rho_{ab}(t) = \frac{\mathrm{i}}{2\pi}\frac{\mu_{ab}}{2\hbar}\int \mathrm{d}t'\mathcal{E}(\vec{r},t')\int \mathrm{d}\omega \mathrm{e}^{\mathrm{i}\omega(t-t')}\frac{\mathrm{i}(\omega-\omega_{ac}-\omega_2)+\gamma_{ac}}{[\mathrm{i}(\omega-\omega_{ab})+\gamma_{ab}][\mathrm{i}(\omega-\omega_{ac}-\omega_2)+\gamma_{ac}]+|\Omega_2|^2}$$

The non-causal contribution, arising from $t'>t$, is obtained by contour integration in the lower-half complex plane. To make the non-causal contribution to vanish, the sum of residues in the lower-half plane must cancel. However, one of the two poles at least must sit in the upper-half plane to give the causal contribution. Therefore if a pole is located in the lower-half plane, the corresponding residue must vanish. One easily checks that $\mathrm{i}(\omega-\omega_{ac}-\omega_2)+\gamma_{ac}$ cannot vanish at a pole sitting in the lower-half plane. Therefore causality imposes that both poles sit in the upper-half plane.

Given the fixed ω_{ac} value, the center of ω_{bc} distribution is located at $\omega_{bc}^{(0)} = \omega_{ab}^{(0)} - \omega_{ac}$. Assuming that the control laser is tuned to resonance with this central frequency, so that $\omega_2 = \omega_{bc}^{(0)}$, substituting Eq. 55 into Eq. 49, and comparing with the susceptibility definition (Eq.52), one finally obtains:

$$\chi^{(+)}(\omega) = -\mathrm{i}\frac{\mu_{ab}^2}{\hbar\epsilon_0}\int \mathrm{d}\omega_{ab} G(\omega_{ab}) \frac{\mathrm{i}(\omega - \omega_{ab}^{(0)}) + \gamma_{ac}}{[\mathrm{i}(\omega - \omega_{ab}) + \gamma_{ab}][\mathrm{i}(\omega - \omega_{ab}^{(0)}) + \gamma_{ac}] + |\Omega_2|^2} \tag{56}$$

The analytical calculation can be completed easily if the atom distribution is given the following Lorentzian form [12]:

$$G(\omega_{ab}) = \frac{n}{\pi}\frac{W_{ab}}{(\omega_{ab} - \omega_{ab}^{(0)})^2 + W_{ab}^2} \tag{57}$$

Summation over ω_{ab} is performed by contour integral. One may notice that the only pole in the upper-half complex plane is located at $\omega_{ab} = \omega_{ab}^{(0)} + \mathrm{i}W_{ab}$. One obtains:

$$\chi^{(+)}(\omega) = -\mathrm{i}n\frac{\mu_{ab}^2}{\hbar\epsilon_0}\frac{\mathrm{i}(\omega - \omega_{ab}^{(0)}) + \gamma_{ac}}{[\mathrm{i}(\omega - \omega_{ab}) + W_{ab} + \gamma_{ab}][\mathrm{i}(\omega - \omega_{ab}^{(0)}) + \gamma_{ac}] + |\Omega_2|^2} \tag{58}$$

Inhomogeneous broadening only results in the substitution of the homogeneous width γ_{ab} with the broadened linewidth $W_{ab} + \gamma_{ab}$. Without further investigation we can conclude that the expressions for induced transparency and reduced group velocity, we previously derived in the absence of inhomogeneous broadening, are still valid provided γ_{ab} is replaced everywhere by $W_{ab} + \gamma_{ab}$. It could be shown easily that Raman transition inhomogeneous broadening is correctly described with substitution of $W_{ac} + \gamma_{ac}$ to γ_{ac}.

5.3 Wave equation in the spectral domain

The temporal picture developed in Section 4 is conditioned by an adiabatic approximation. The present spectral analysis, not limited by such condition, is worth visiting a little further.

In the spectral domain the wave equation reads as:

$$\Delta\hat{E}(\vec{r},\omega) + \frac{\omega^2}{c^2}\hat{E}(\vec{r},\omega) = -\omega^2\mu_0\hat{P}(\vec{r},\omega) \tag{59}$$

The polarization density being expressed in terms of susceptibility, the wave equation for the positive frequency field component reads as:

$$\Delta\hat{\mathcal{E}}(\vec{r},\omega) + \frac{\omega^2}{c^2}\left[1+\chi^{(+)}(\omega)\right]\hat{\mathcal{E}}(\vec{r},\omega) = 0 \tag{60}$$

The field is assumed to be a plane wave propagating along Oz. One looks for a solution in the form $\hat{\mathcal{E}}(\vec{r},\omega) = \underline{\mathcal{E}}(\omega)\mathrm{e}^{-i\kappa z}$. The wave equation then reduces to:

$$\left(\frac{\omega^2}{c^2}\left[1+\chi^{(+)}(\omega)\right] - \kappa^2\right)\underline{\mathcal{E}}(\omega) = 0 \tag{61}$$

With $\kappa = k' - \mathrm{i}\alpha/2$, the solution is given by:

$$\begin{aligned} k'^2 - \frac{\alpha^2(\omega)}{4} &= k^2\left[1+\chi_r^{(+)}(\omega)\right] \\ \alpha(\omega) &= -\frac{k^2}{k'^2}\chi_{im}^{(+)}(\omega) \end{aligned} \tag{62}$$

where $\chi_r^{(+)}(\omega)$ and $\chi_{im}^{(+)}(\omega)$ respectively stand for the real and imaginary part of $\chi^{(+)}(\omega)$. Under the assumption that $\left|\chi_r^{(+)}(\omega)\right| << 1$ and $\alpha(\omega) << \omega/c$, the wave vector k' and the absorption coefficient $\alpha(\omega)$ read as:

$$\begin{aligned} k'(\omega) &= \frac{\omega}{c}\sqrt{1+\chi_r^{(+)}(\omega)} \\ \alpha(\omega) &= -k\chi_{im}^{(+)}(\omega) \end{aligned} \tag{63}$$

Substituting Eq. 58 into Eq. 63, one easily recovers the previously obtained expression of opacity at resonance. In the same way one can calculate the velocity group at resonance, given the definition as $v = (\mathrm{d}k'/\mathrm{d}\omega)^{-1}$.

More interestingly, the off-resonance regime can be explored. Disregarding inhomogeneous broadening, and expanding susceptibility to second order as a function of detuning, one can express the transmitted power spectrum $I(z=L,\omega)$ as:

$$I(z=L,\omega) = I(z=0,\omega)\exp\left\{-\alpha_0 L\left(\frac{\gamma_{ac}\gamma_{ab}}{|\Omega_2|^2} + \left[\frac{(\omega-\omega_{ab})\gamma_{ab}}{|\Omega_2|^2}\right]^2\right)\right\} \tag{64}$$

which leads to a gaussian-shape transparency window whose width agrees with Eq. 38.

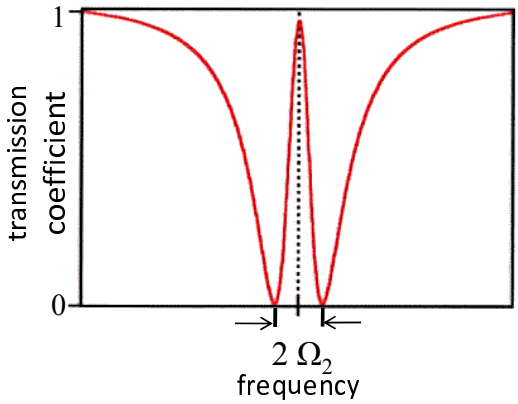

Figure 5: EIT transmission profile exhibiting the Autler Townes doublet.

5.4 Memory bandwidth

In the prospect of signal processing applications, the transparency width is a critical parameter. This quantity has been derived above by limited order expansion of the susceptibility, but we need not restrict to this small detuning region. Considering Eq. 58, one observes that, in conditions required for the opening of the transparency window, when $|\Omega_2|^2 >> (W_{ab}+\gamma_{ab})\gamma_{ac}$, $\chi^{(+)}(\omega)$ exhibits quasi-singularities at $\omega - \omega_{ab}^{(0)} = \pm|\Omega_2|$ (see Fig. 5). One easily verifies that, at these spectral positions, the absorption coefficient returns to its maximum value α_0. Those two absorptions peaks reflect the Autler-Townes splitting of level b. Therefore the transparency width appears to be limited by the control field Rabi frequency.

This result also gives some information on the validity range of Eq. 64. Transparency width limitation to $|\Omega_2|$ requires that $\Delta_T < |\Omega_2|$, where Δ_T is given by Eq. 38. This is consistent with $\Delta_T < |\Omega_2| < \gamma_{ab}\sqrt{\alpha_0 L}$, which corresponds to a transparency window narrower than the absorption profile.

One might be tempted to increase the control field Rabi frequency in order to improve the memory operation bandwidth. However one must keep in mind that a small velocity group is necessary for efficient information transfer from the signal field to the Raman coherence. Under condition $|\Omega_2| < \gamma_{ab}\sqrt{\alpha_0 L}$, the transparency width can be expressed in terms of the group velocity as:

$$\Delta_T = 2v\sqrt{\alpha_0/L}, \tag{65}$$

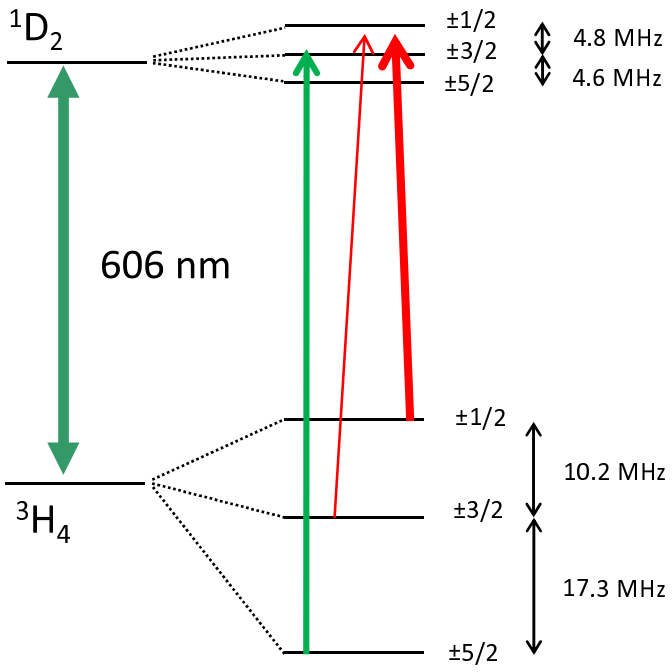

Figure 6: Three-level Λ-system in $Pr^{3+} : Y_2SiO_5$. In addition to the two fields involved in the EIT process, a third beam is used to repump ions from the $^3H_4(\pm 5/2)$ ground state sublevel. Repumping serves to select the active ions within a narrow spectral interval, thus reducing the effective inhomogeeous width.

which depends neither on the absorption linewidth nor on the Rabi frequency.

Finally it should be noticed that, if Raman transition too is affected by inhomogeneous broadening, then the group velocity lower bound is deteriorated, increasing from γ_{ac}/α_0 to W_{ac}/α_0.

5.5 EIT demonstration in solids

The EIT process was observed for the first time in a rare earth ion doped crystal of $Pr^{3+} : Y_2SiO_5$ in 1997 [13]. Experiment operated on transition $^1D_2 -^3 H_4$ at $606nm$ (see Fig. 6). With a $I = 5/2$ nuclear spin, each electronic level is six times degenerate. Hyperfine interaction lifts degeneracy into 3 pairs of sub-levels, with a splitting in the MHz range. A Λ system is

obtained when two lower sublevels are connected by optical transition to a common upper sub-level.

Inhomogeneous broadening reaches $W_{ab} = 4GHz$. This is much larger than the optical homogeneous width and the sub-level spacing and does not satisfy the inhomogeneous broadening conditions of the calculation in section 5.2. Indeed we performed this calculation under assumption that $W_{ab} << \omega_{ac}$.

Actually, a preparation step artificially reduces the effective inhomogeneous broadening to make it consistent with the above calculation. The two fields involved in the EIT process optically pump the ions to the third ground sublevel that plays the role of a shelving state. The absortion profile is thus totally bleached over the spectral interval within reach of the EIT fields. A narrow absorption band is then restored by a monochromatic repump beam that returns a specific spectral class of ions from the shelving state to $|a\rangle$ state. The width of this group of ions, limited by the repump laser linewidth, represents the effective inhomogeneous broadening W_{ab}^{eff} that easily satisfies the condition $W_{ab}^{eff} << \omega_{ac}$.

One may wonder about the contribution from ions, far from optical resonance, but still satisfying the two-photon transition resonance condition. Actually only ions with unbalanced sublevel population can contribute to a two-photon process such as EIT, since the Raman transition probability is proportional to the sublevel population difference. Far from optical excitation by the different fields, the sublevels are equally populated at thermal equilibrium and those ions can be ignored.

The Raman transition is affected by a $\approx 50kHz$ inhomogeneous broadening in $Pr^{3+} : Y_2SiO_5$. This broadening should be subsituted to γ_{ac} in the EIT process description. Finally, a $60kHz$-wide EIT transparency window was observed.

Observation of EIT was reported in various other solid state materials such as semiconductors [14, 15], nitrogen-vacancy color centers in diamond [16], Nd^{3+}-doped crystals [17] but, for the time being, $Pr^{3+} : Y_2SiO_5$ still by far outgoes these systems in terms of Raman coherence lifetime or EIT efficiency.

Stopped light was also demonstrated in a Pr^{3+}-doped crystal [18], with a memory lifetime of a few hundreds of μs. The storage lifetime was then dramatically increased to more than $1s$ by an Australian group [19]. All these works have been performed with classical light. Quantum light storage

in a solid has yet to be observed.

6 Recovery from an absorbing medium

In EIT the operation bandwidth, given by the transparency window, is directly related to the control field Rabi frequency. At storage and retrieval both the signal and the control fields have to be present simultaneously within the memory. We now consider an alternative protocol, first proposed in Ref.[20], and examined in further details in [21]. This is based on direct absorption. The signal to be stored interacts alone with the active material. The operation bandwidth is expected to be related to the absorption linewidth.

6.1 Polarization collapse, coherence survival

As already noticed in section 2.2, since information has to be stored first into the optical coherence ρ_{ab}, the information carrier pulse duration must be much smaller than the inverse homogeneous width γ_{ab}. Hence the pulse spectral width must be much larger than γ_{ab}. In addition, since storage is based on absorption, the pulse must be narrower than the absorption profile. In an homogeneously broadened medium, where all atoms have the same transition frequency, the absorption linewidth is given by $\gamma_{ab}\sqrt{\alpha_0 L}$. Hence one is left with the very restrictive condition $\sqrt{\alpha_0 L} >> 1$, similar to the one already met in the frame of EIT. Interestingly, the condition can be easily relaxed in inhomogeneously broadened material where the absorption width can by far exceed $\gamma_{ab}\sqrt{\alpha_0 L}$. In the following we thus restrict the discussion to inhomogeneously broadened media. One may notice that, in EIT regime, the condition $\sqrt{\alpha_0 L} >> 1$ prevails whether the line is inhomogeneously broadened or not.

The atomic response to a weak pulse was considered already in the frame of EIT. To describe simple absorption one just cancels Ω_2 in Eq. 56 and obtains:

$$\chi^{(+)}(\omega) = -\mathrm{i}\frac{\mu_{ab}^2}{\hbar\epsilon_0}\int \mathrm{d}\omega_{ab} G(\omega_{ab})\frac{1}{\mathrm{i}(\omega-\omega_{ab})+\gamma_{ab}} \tag{66}$$

Assuming the homogeneous line is much narrower than $G(\omega_{ab})$, one simplifies

$\chi^{(+)}(\omega)$ into:

$$\chi^{(+)}(\omega) = -\mathrm{i}\pi \frac{\mu_{ab}^2}{\hbar\epsilon_0} G(\omega) \tag{67}$$

and the atomic response, as given by the polarization density, reads as (see Eq. 52):

$$\hat{P}(\vec{r},\omega) = \frac{1}{2}\epsilon_0 \left[\chi^{(+)}(\omega)\hat{\mathcal{E}}(\vec{r},\omega) + \chi^{(-)}(\omega)\hat{\mathcal{E}}^*(\vec{r},-\omega)\right] \tag{68}$$

Since the inhomogeneous distribution $G(\omega)$ is assumed to be much broader than the incoming pulse spectrum, the above equation tells us that the atomic response matches the incoming pulse in the spectral domain. Therefore temporal profiles coincide too. In other words the material response does not survive to the incoming pulse, collapsing as the field drops to zero. The instantaneous character of the material response is the reason why the pulse propagation is just reflected by an attenuation factor.

However, provided the homogeneous width is much smaller than the inverse pulse duration, the atomic coherences subsists long after the pulse has faded away. This is confirmed by the integral Bloch equation. According to Eq. 10, to first order in the field amplitude, assuming all atoms are initially in state $|a\rangle$, one obtains :

$$\rho_{ab}(\omega_{ab};\vec{r},t) = \mathrm{i}\frac{\mu_{ab}}{2\hbar}\int_{-\infty}^{t} dt' \mathcal{E}(\vec{r},t')\mathrm{e}^{(\mathrm{i}\omega_{ab}-\gamma_{ab})(t-t')} \tag{69}$$

The coherence, built by the incoming pulse, relaxes with rate γ_{ab} and may survive long after the field has vanished. The origin of the polarization density collapse lies in the phase shift of the different atoms distributed over the inhomogeneously broadened absorption profile. This is reflected in the above equation by the ω_{ab}-dependent phase factor that keeps on building up after the pulse extinction. As a result, the different atom contributions interfere destructively as they are combined into the polarization density.

In order to extract the information stored in the atomic coherences, one has to rephase them. We shall demonstrate that phase reversal makes the coherences to faithfully regenerate the initial light pulse.

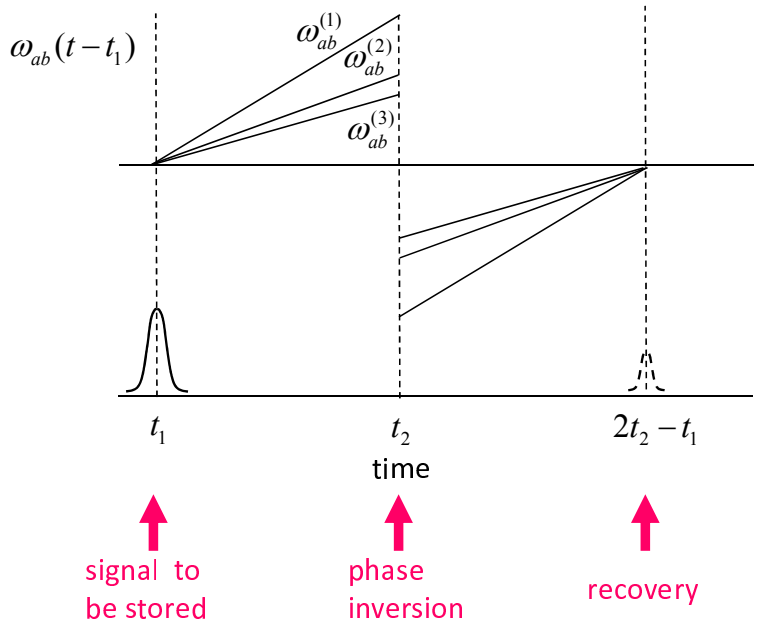

Figure 7: Rephasing. All the atoms have the same phase at t_1. Then phase shift accumulates between atoms with different transition frequencies. At t_2 the phase is reversed so that all atoms are phased together again at $2t_2 - t_1$

6.2 Information recovery by phase reversal

Let us assume that at time t_2, after the extinction of the incoming pulse, one is able to achieve the following phase reversal operation:

$$\rho_{ab}(\omega_{ab}; \vec{r}, t_2^{(+)}) = \rho_{ba}(\omega_{ab}; \vec{r}, t_2^{(-)}) \tag{70}$$

In addition we assume that the operation does not entail any level population change, a condition that will prove mostly important and difficult to satisfy practically. Enacting the rule for ρ_{ab} instead of $\tilde{\rho}_{ab}$, we mean reversal affects both the spatial and the spectral phase. At t_2 both transformations $kz \to -kz$ and $\omega_{ab}(t_2 - t_1) \to -\omega_{ab}(t_2 - t_1)$ shall occur.

This phase reversal procedure is pure speculation so far. Later on we shall examine practical means to achieve this operation.

After t_2, the spectral phase keeps on growing at the same rate, in such a way that at time $t = 2t_2 - t_1$ the phase shift $\omega_{ab}(t + t_1 - t_2)$ simultaneously vanishes in all the atoms, whatever their transition frequency (see Fig. 7).

Being phased together, the atoms radiate a light pulse at that moment. In an optically thin sample we could consider that the coherences just evolve freely, independently from each other. The feedback of the radiated pulse on the atoms would remain weak with respect to the initial pulse. On the contrary we are dealing with an optically thick, opaque medium. We can no longer neglect the radiated response feedback. Indeed the delayed radiated response will prove to reach the same amplitude as the initial incoming pulse. Such a feedback is not unfamiliar to us. We implicitly accounted for such a reaction when we derived the incoming pulse wave equation: each atom undergoes excitation by a local field that combines the input field and the contributions of the upstream atoms. In order to calculate the restored field and the final atomic state, we take the usual steps, first deriving the individual atom response from the Bloch equation, then combining the elementary coherences into the macroscopic polarization density, that is finally used as a source term in the wave equation to be satisfied by the restored field.

Let $\mathcal{E}_{out}(\vec{r},t)$ denote the field radiated by the atoms after t_2. At $t > t_2$, the Bloch equation for coherences reads as:

$$\rho_{ab}(\omega_{ab};\vec{r},t) = \rho_{ab}(\omega_{ab};\vec{r},t_2^{(+)})\mathrm{e}^{(\mathrm{i}\omega_{ab}-\gamma_{ab})(t-t_2)} + \mathrm{i}\frac{\mu_{ab}}{2\hbar}\int_{t_2}^{t} dt'\mathcal{E}_{out}(\vec{r},t')\mathrm{e}^{(\mathrm{i}\omega_{ab}-\gamma_{ab})(t-t')} \tag{71}$$

The two terms on the right hand side respectively correspond to the free evolution of the initial coherence and to the radiated response feedback on the coherences.

Since atoms evolve freely from initial excitation by $\mathcal{E}_{in}(\vec{r},t)$ to time t_2, the coherence at t_2 is simply given by:

$$\rho_{ab}(\omega_{ab};\vec{r},t_2^{(-)}) = \mathrm{i}\frac{\mu_{ab}}{2\hbar}\int_{-\infty}^{t_2} dt'\mathcal{E}_{in}(\vec{r},t')\mathrm{e}^{(\mathrm{i}\omega_{ab}-\gamma_{ab})(t-t')} \tag{72}$$

Taking account of the reversal rule (Eq. 70) and substituting into Eq. 71, one obtains:

$$\rho_{ab}(\omega_{ab};\vec{r},t) = -\mathrm{i}\frac{\mu_{ab}}{2\hbar}\left[\int_{-\infty}^{t_2}\mathrm{d}t'\mathcal{E}_{in}^{*}(\vec{r},t')\mathrm{e}^{\mathrm{i}\omega_{ab}(t+t'-2t_2)-\gamma_{ab}(t-t')} - \int_{t_2}^{t} dt'\mathcal{E}_{out}(\vec{r},t')\mathrm{e}^{(\mathrm{i}\omega_{ab}-\gamma_{ab})(t-t')}\right] \tag{73}$$

The polarization density $P(\vec{r},t)$is obtained by substitution of Eq. 73 into Eq. 48. The positive frequency component of $P(\vec{r},t)$ can be split in two terms

$P_1^{(+)}(\vec{r},t)$ and $P_2^{(+)}(\vec{r},t)$ according to:

$$P^{(+)}(\vec{r},t) = P_1^{(+)}(\vec{r},t) + P_2^{(+)}(\vec{r},t) \tag{74}$$

where $P_1^{(+)}(\vec{r},t)$ and $P_2^{(+)}(\vec{r},t)$ respectively correspond to the atom free evolution from t_2 and to the recovered field feedback on the atoms. The first term reads as:

$$P_1^{(+)}(\vec{r},t) = \mathrm{i}\frac{\mu_{ab}^2}{2\hbar}\int_{-\infty}^{t_2} \mathrm{d}t' \mathcal{E}_{in}^*(\vec{r},t')\mathrm{e}^{-\gamma_{ab}(t-t')} \int \mathrm{d}\omega_{ab} G(\omega_{ab})\mathrm{e}^{\mathrm{i}\omega_{ab}(t+t'-2t_2)} \tag{75}$$

Since the field spectrum is assume to be much narrower than $G(\omega_{ab})$, the quantity $\mathcal{E}_{in}^*(\vec{r},t')\mathrm{e}^{\mathrm{i}\omega_L t'}$ varies slowly with respect to $\int \mathrm{d}\omega_{ab} G(\omega_{ab})\mathrm{e}^{\mathrm{i}\omega_{ab}(t+t'-2t_2)}$ that peaks abruptly at $t' = 2t_2 - t$. Taking $\mathcal{E}_{in}^*(\vec{r},t')\mathrm{e}^{\mathrm{i}\omega_L t'}\mathrm{e}^{-\gamma_{ab}(t-t')}$ out of the sum over t' at $t' = 2t_2 - t$, one obtains:

$$P_1^{(+)}(\vec{r},t) = 2\mathrm{i}\pi\frac{\mu_{ab}^2}{2\hbar} G(\omega_L)\mathcal{E}_{in}^*(\vec{r},2t_2-t)\mathrm{e}^{-2\gamma_{ab}(t-t_2)} \tag{76}$$

Fourier transformation to frequency domain leads to:

$$\hat{P}_1^{(+)}(\vec{r},\omega) = 2\mathrm{i}\pi\frac{\mu_{ab}^2}{2\hbar} G(\omega_L)\hat{\mathcal{E}}_{in}^*(\vec{r},\omega)\mathrm{e}^{-2\mathrm{i}\omega t_2 - 2\gamma_{ab}(t_2-t_1)} \tag{77}$$

As for the second term $P_2^{(+)}(\vec{r},t)$, we can proceed directly to its frequency domain expression. Indeed this term simply describes the linear response to $\mathcal{E}_{out}(\vec{r},t)$, as given by Eqs 67 and 52:

$$\hat{P}_2^{(+)}(\vec{r},\omega) = -\mathrm{i}\pi\frac{\mu_{ab}^2}{2\hbar} G(\omega_L)\hat{\mathcal{E}}_{out}(\vec{r},\omega) \tag{78}$$

The two terms $\hat{P}_1^{(+)}(\vec{r},\omega)$ and $\hat{P}_2^{(+)}(\vec{r},\omega)$ finally combine into the positive frequency component of the polarization density as:

$$\hat{P}^{(+)}(\vec{r},\omega) = -\mathrm{i}\pi\frac{\mu_{ab}^2}{2\hbar} G(\omega_L)\left[\hat{\mathcal{E}}_{out}(\vec{r},\omega) - 2\hat{\mathcal{E}}_{in}^*(\vec{r},\omega)\mathrm{e}^{-2\mathrm{i}\omega t_2 - 2\gamma_{ab}(t_2-t_1)}\right] \tag{79}$$

This quantity can be substituted into the wave equation for the restored field:

$$\frac{1}{2}\left(\frac{\partial^2}{\partial z^2} + k^2\right)\hat{\mathcal{E}}_{out}(\vec{r},\omega) = -\omega^2\mu_0\hat{P}^{(+)}(\vec{r},\omega) \tag{80}$$

We look for a solution in the form $\hat{\mathcal{E}}_{out}(\vec{r},\omega) = A(z,\omega)\mathrm{e}^{\mathrm{i}kz}$, counterpropagating with the incoming field $\hat{\mathcal{E}}_{in}(\vec{r},\omega)$. Indeed, given the form of $\hat{P}^{(+)}(\vec{r},\omega)$, the restored field is a function of $\hat{\mathcal{E}}^*_{in}(\vec{r},\omega)$, a field that varies as $\mathrm{e}^{\mathrm{i}kz}$. The linearized wave equation finally reads as:

$$\frac{\partial}{\partial z}A(z,\omega) = \frac{1}{2}\alpha_0\left[A(z,\omega) - 2\hat{\mathcal{E}}^*_{in}(\vec{r},\omega)\mathrm{e}^{-2\mathrm{i}\omega t_2 - 2\gamma_{ab}(t_2-t_1)-\mathrm{i}kz}\right] \tag{81}$$

where:

$$\alpha_0 = \frac{\pi k \mu_{ab}^2}{2\hbar\epsilon_0}G(\omega_L) \tag{82}$$

With the boundary condition $A(L,\omega) = 0$ at the output side $z = L$ of the absorbing medium, and the incoming field spatial distribution $\hat{\mathcal{E}}^*_{in}(z,\omega) = \mathcal{E}^*_{in}(0,\omega)\mathrm{e}^{-\frac{1}{2}\alpha_0 z + \mathrm{i}kz}$, expressed in terms of the amplitude in the input side at $z = 0$, one easily[3] gets the solution as:

$$\hat{\mathcal{E}}_{out}(z,\omega) = \hat{\mathcal{E}}^*_{in}(z,\omega)\mathrm{e}^{-2\mathrm{i}\omega t_2 - 2\gamma_{ab}(t_2-t_1)}\left[1 - \mathrm{e}^{\alpha_0(L-z)}\right] \tag{83}$$

Inverse Fourier transformation leads to the following solution in the time domain:

$$\mathcal{E}_{out}(z,t) = \mathcal{E}^*_{in}(z,2t_2-t)\mathrm{e}^{-2\gamma_{ab}(t_2-t_1)}\left[1 - \mathrm{e}^{\alpha_0(L-z)}\right] \tag{84}$$

Since $\mathcal{E}^*_{in}(z,2t_2-t)$ is centered at t_1, the recovered signal emission is centered at $2t_2 - t_1$ as expected. Otherwise, the restored field envelope is time reversed with respect to the initial pulse. Finally, the field amplitude is exactly restored at $z = 0$ provided $\alpha_0 L >> 1$.

We assumed the phase reversal operation does not increase the upper level population. In the opposite limit, let us assume that a side effect of the phase reversal operation is to promote all atoms to the upper level. Then the storage material becomes an amplifier, with gain equal to $\alpha_0 L$ for the regenerated field emerging from the input side. Such an amplification certainly modifies the quantum properties of the restored field. In addition amplified spontaneous emission then deteriorates the restitution fidelity.

[3] With the change of variable: $A(z,\omega) = B(z,\omega)\mathrm{e}^{\alpha_0 z/2}$, the wave equation is turned into: $\partial_z B(z,\omega) = -\alpha_0\hat{\mathcal{E}}^*_{in}(0,\omega)\mathrm{e}^{-\alpha_0 z - 2\mathrm{i}\omega t_2 - 2\gamma_{ab}(t_2-t_1)}$. Summing from z to L with boundary condition $B(L,\omega) = 0$, one obtains: $B(z,\omega) = \hat{\mathcal{E}}^*_{in}(0,\omega)\mathrm{e}^{-2\mathrm{i}\omega t_2 - 2\gamma_{ab}(t_2-t_1)}\left(\mathrm{e}^{-\alpha_0 z} - \mathrm{e}^{-\alpha_0 L}\right)$

Substitution of the restored field in Eq. 73 leads to:

$$\rho_{ab}(\omega_{ab};\vec{r},t) = -\mathrm{i}\frac{\mu_{ab}}{2\hbar}\mathrm{e}^{-\gamma_{ab}(t-t_1)}\left[\int_{-\infty}^{2t_2-t}\mathrm{d}t'\mathcal{E}^*_{in}(\vec{r},t')\mathrm{e}^{\mathrm{i}\omega_{ab}(t+t'-2t_2)}\right.$$
$$\left.+\mathrm{e}^{-\alpha_0(L-z)}\int_{2t_2-t}^{t_2}dt'\mathcal{E}^*_{in}(\vec{r},t')\mathrm{e}^{\mathrm{i}\omega_{ab}(t+t'-2t_2)}\right] \quad (85)$$

As expected, the coherence drops to zero whilst the light pulse is being restored, around $t = 2t_2 - t_1$. Indeed, during the recovery step, each atom is exposed to excitation coming up from the downstream atoms, that is to say from atoms located further from the input side. This radiation gives a kick in direction opposite to the initial pulse effect, making the atom return to the initial state. Closer to the input side, the restored signal acting on atoms grows bigger, precisely where the atoms were exposed to larger excitation by the initial pulse. A long time after $t = 2t_2 - t_1$, the coherence reduces to:

$$\rho_{ab}(\omega_{ab};z,t) = -\mathrm{i}\frac{\mu_{ab}}{2\hbar}\mathrm{e}^{-\alpha_0(L-\frac{1}{2}z)}\hat{\mathcal{E}}^*_{in}(0,\omega_{ab})\mathrm{e}^{\mathrm{i}\omega_{ab}(t-2t_2)}\mathrm{e}^{-\gamma_{ab}(t-t_1)} \quad (86)$$

which expresses the $\alpha_0 L$ dependence of the residual excitation.

During the storage process, a part $W/W_{in} = (1 - \mathrm{e}^{-\alpha_o L})$ of the incoming energy stays in the medium, the remaining passing through without being absorbed. From the part that is stored, a fraction is lost at retrieval, even in the absence of dipole relaxation. Indeed the restored field is $(1 - \mathrm{e}^{-\alpha_o L})$ times smaller than the incoming one, according to Eq. 84. Therefore one recovers a fraction $W_{out}/W_{in} = (1 - \mathrm{e}^{-\alpha_o L})^2$ of the incoming energy. The energy $W - W_{out} \cong W_{in}\mathrm{e}^{-\alpha_o L}$ remains within the material. To summarize, with a finite length material, energy is lost in equal amounts at storage and retrieval, one part being transmitted without absorption, the other part being left as an atomic excitation.

7 Practical implementation of phase reversal

The signal recovery procedure examined in the previous section requires:

- spectral phase reversal of the optical coherence in all the atoms simultaneously at a given time
- spatial phase reversal of the optical coherence in all the atoms

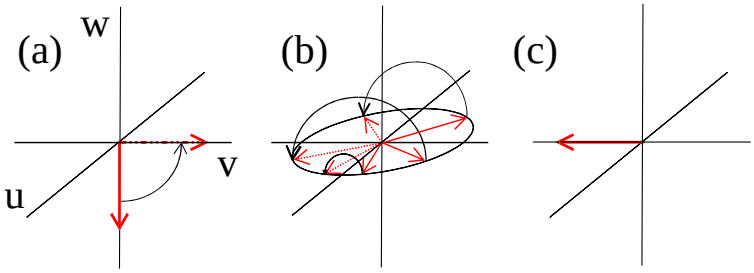

Figure 8: Two-pulse echo. (a) At time t_1 a $\pi/2$-pulse brings the Bloch vectors of all frequency classes along Ov. (b) The Bloch vectors spread over the equatorial plane and at time t_1+t_{12} a π-pulse reverses their v coordinate. (c) At time t_1+2t_{12} all the Bloch vectors are back along Ov.

- no excitation to the upper level during the phase reversal process

We review different practical phase reversal procedures and check their ability to satisfy the above conditions.

7.1 Two-pulse photon echo

Phase reversal has been actively investigated for several decades, first in the framework of NMR, then in the optical domain after the advent of the laser. Known as *spin echo* in NMR and *photon echo* in optics, this phenomenon is best described in the Bloch vector picture (see Appendix B).

Let an inhomogeneously broadened ensemble of two-level atoms be illuminated at time t_1 by a light pulse of duration τ and Rabi frequency Ω_1. Under assumption that Ω_1 is real, the driving vector $\vec{\beta}$ is directed along Ou. Let the pulse be too short for the inhomogeneous phase to build up during the pulse. In other words the detuning $\Delta = \omega_{ab} - \omega_L$ is assumed to be much smaller than τ^{-1}. Then, driven by the applied field, the Bloch vector precesses around $\vec{\beta}$ at angular velocity Ω_1. The quantity $\int_{-\infty}^{+\infty} \Omega_1(t')\mathrm{d}t'$, known as the *pulse area*, represents the angle travelled by the Bloch vector around Ou during the pulse. Initially the Bloch vector is directed downward along the Bloch sphere vertical axis Ow. Let the pulse area equal $\pi/2$. Then the pulse makes the Bloch vector to travel a $\pi/2$ angle around Ou and brings it along Ov, in the equatorial plane of the Bloch sphere, as shown in Fig. 8.

After the $\pi/2$-pulse extinction, the Bloch vector precesses around the

vertical axis Ow at velocity Δ. At time t the Bloch vector coordinates read as:

$$\begin{cases} u(t) &= \sin[\Delta(t-t_1)]\mathrm{e}^{-\gamma_{ab}(t-t_1)} \\ v(t) &= \cos[\Delta(t-t_1)]\mathrm{e}^{-\gamma_{ab}(t-t_1)} \\ w(t) &= 0 \end{cases} \tag{87}$$

where the population relaxation has been neglected. The Bloch vectors belonging to different frequency classes rotate at different angular velocities Δ and, as time elapses, they depart from each other, generating a "pancake" that spreads over the Bloch sphere equatorial plane.

At time t_2 a second pulse is applied. Let the pulse area equal π. Therefore each Bloch vector is made to travel a π angle around Ou, returning to the equatorial plane with reversed v coordinate. Just after the second pulse the Bloch vector coordinates read as:

$$\begin{cases} u(t_2) &= \sin[\Delta t_{12}]\mathrm{e}^{-\gamma_{ab}t_{12}} \\ v(t_2) &= -\cos[\Delta t_{12}]\mathrm{e}^{-\gamma_{ab}t_{12}} \\ w(t_2) &= 0 \end{cases} \tag{88}$$

This represents a symmetry with respect to the plane uOw. The slowest frequency classes find themselves in advance of the fastest ones. As time elapses, the free evolution is depicted by:

$$\begin{cases} u(t) &= \{u(t_2)\cos[\Delta(t-t_2)] + v(t_2)\sin[\Delta(t-t_2)]\}\,\mathrm{e}^{-\gamma_{ab}(t-t_1)} \\ v(t) &= \{-u(t_2)\sin[\Delta(t-t_2)] + v(t_2)\cos[\Delta(t-t_2)]\}\,\mathrm{e}^{-\gamma_{ab}(t-t_1)} \\ w(t) &= 0 \end{cases} \tag{89}$$

The fastest vectors catch up the slowest ones so that they all meet along -Ov at time $2t_2 - t_1$, according to:

$$\begin{cases} u(2t_2-t_1) &= 0 \\ v(2t_2-t_1) &= -\mathrm{e}^{-2\gamma_{ab}t_{12}} \\ w(2t_2-t_1) &= 0 \end{cases} \tag{90}$$

At that moment the dipoles are phased together and emit the photon echo signal.

In the context of our quest for phase reversal, it is worth noticing the transformation undergone at t_2 can be expressed, in terms of coherence, as:

$$\tilde{\rho}_{ab}(t_2^{(+)}) = \tilde{\rho}_{ba}(t_2^{(-)}) \tag{91}$$

In the above discussion we have implicitly supposed that both pulses propagate in the same direction. If pulses propagate in different direction one must notice that the change of variable $\rho_{ab} \rightarrow \tilde{\rho}_{ab}$ depends on the wave vector of the reference pulse. Just before the second pulse the change of variable is still referred to the first pulse and reads as:

$$\rho_{ab}(t_2^{(-)}) = \tilde{\rho}_{ab}(t_2^{(-)})\mathrm{e}^{\mathrm{i}(\omega_L t_2 - \vec{k}_1.\vec{r})} \tag{92}$$

According to Eq. 91, at t_2 the coherence, this time referred to the second pulse, undergoes the transformation:

$$\tilde{\rho}_{ab}(t_2^{(+)}) = \tilde{\rho}_{ba}(t_2^{(-)}) \tag{93}$$

or, equivalently, in terms of ρ_{ab} :

$$\rho_{ab}(t_2^{(+)}) = \rho_{ba}(t_2^{(-)})\mathrm{e}^{2\mathrm{i}(\omega_L t_2 - \vec{k}_2.\vec{r})} \tag{94}$$

Then, substituting Eq. 92 in this expression one finally obtains:

$$\rho_{ab}(t_2^{(+)}) = \tilde{\rho}_{ba}(t_2^{(-)})\mathrm{e}^{\mathrm{i}\left[\omega_L t_2 - (2\vec{k}_2 - \vec{k}_1).\vec{r}\right]} \tag{95}$$

where $\tilde{\rho}_{ba}(t_2^{(-)})$ is a slowly varying function of $\vec{r}$. The space-dependent phase factor indicates that the echo signal is emitted in direction $2\vec{k}_2 - \vec{k}_1$. Dipole contributions are phase-matched all along the sample of length L provided: $\left(|2\vec{k}_2 - \vec{k}_1| - k\right) L << \pi$. As soon as L exceeds a few hundreds of wavelengths, the condition is satisfied only when $\vec{k}_2$ is close to $\vec{k}_1$, which leads to emission in direction close to $\vec{k}_1$ and $\vec{k}_2$.

The second pulse in the photon echo sequence reverses the phase of $\tilde{\rho}_{ab}$ (see Eq. 91), not that of ρ_{ab}, as requested in section 6.2. Therefore, the spectral phase reversal requirement is satisfied, as illustrated by the coherence rephasing leading to echo emission, but spatial phase reversal is missing. The phase matching condition forcing echo emission in forward direction reflects the absence of spatial phase reversal.

Another condition is not satisfied. In the photon echo memory protocol, the information to be stored should be carried by the first pulse while the second pulse would be devoted to phase inversion. Initially all atoms are prepared in the ground state. The Bloch vector is vertical, downward oriented. Unlike the $\pi/2$ pulse we considered in the brief presentation of photon

echo, the weak signal pulse, with an area much smaller than unity, hardly displaces the Bloch vector from its initial vertical direction. The second pulse is expected to convert $\tilde{\rho}_{ab}$ into $\tilde{\rho}_{ba}$, which corresponds to a reflection in the vertical plane uOw. But light cannot perform such a transformation! Light can only rotate the Bloch vector around an horizontal axis. Now the product of two reflections is actually equivalent to a rotation around the intersection of the two planes of symmetry. Given one of the symmetries is taken with respect to uOw, the other reflection plane will have to intersect uOw along the rotation axis. The only symmetry that preserves the phase inversion is the reflection with respect to the equatorial plane uOv, orthogonal to uOw. Combining those two symmetries corresponds to a π-rotation that keeps the Bloch vector nearly vertical, but now pointing up. In other words, the second pulse, in order to accomplish the expected spectral phase inversion, shall also promote all the atoms to the upper level. As already noticed, this would deeply affect the restored signal.

In conclusion, the two-pulse photon echo protocol fails to satisfy two out of the three signal recovery requirements.

7.2 Tri-level echo

The photon echo process is easily extended to the three-level Λ-system we already met in EIT [22]. As in EIT, information is stored in the Raman coherence but, unlike EIT, a single transition is excited at a time.

Let the system be illuminated by a three-pulse sequence. The time-separated driving pulses alternatively excite the $a \rightarrow b$ and $b \rightarrow c$ transitions. All the atoms have been prepared initially in state $|a\rangle$. By exciting the $a \rightarrow b$ transition, the first pulse builds the optical coherence ρ_{ab}. The second pulse, resonant with the $b \rightarrow c$ transition, converts ρ_{ab} into the ρ_{ac} Raman coherence. Then a third pulse excites $a \rightarrow b$ again, converting ρ_{ac} into the ρ_{bc} optical coherence that gives rise to the tri-level echo (see Fig. 9).

Interaction with the first pulse does not need much comment. Only states $|a\rangle$ and $|b\rangle$ are implied at this stage. The system obeys the two-level Bloch equation. After the pulse extinction the coherence $\tilde{\rho}_{ab}(\omega_{ab}; \vec{r}, t_1)$ evolves freely to $\tilde{\rho}_{ab}(\omega_{ab}; \vec{r}, t) = \tilde{\rho}_{ab}(\omega_{ab}; \vec{r}, t_1)\mathrm{e}^{(\mathrm{i}\Delta - \gamma_{ab})(t-t_1)}$, where $\Delta = \omega_{ab} - \omega_1$. Interaction with second pulse must be examined more carefully since the three levels are now involved. Since a single transition is excited, Eq.26 splits into two

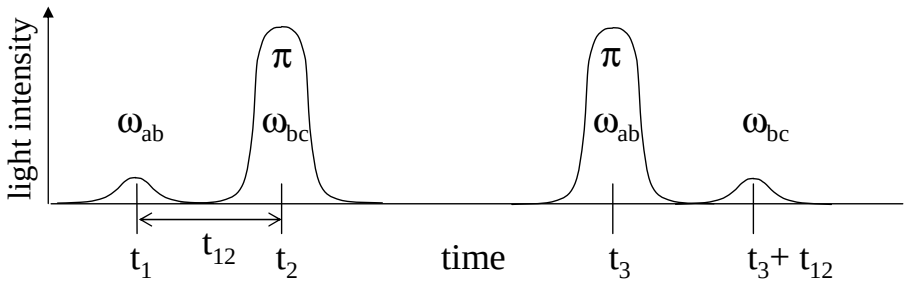

Figure 9: tri-level echo in a Λ-system. The first two pulses build the Raman coherence ρ_{ac} from the optical coherence ρ_{ab}. The inhomogeneous phase shift accumulated by ρ_{ab} between t_1 and t_2 is carried to ρ_{ac} between t_2 and t_3. Then ρ_{ac} is turned into ρ_{bc} by the third pulse. The inhomogeneous phase shift vanishes at t_3, which gives rise to echo emission.

uncoupled sets of equations:

$$\left\{ \begin{array}{ll} \dot{\rho}_{cc} & = \frac{\mathrm{i}}{2}(\tilde{\rho}_{cb}\Omega_2^* - \tilde{\rho}_{bc}\Omega_2) \\ \dot{\rho}_{bb} & = -\dot{\rho}_{cc} \\ \dot{\tilde{\rho}}_{cb} & = \frac{\mathrm{i}}{2}(\rho_{cc} - \rho_{bb})\Omega_2 \end{array} \right. \tag{96}$$

and

$$\left\{ \begin{array}{ll} \dot{\tilde{\rho}}_{ab} & = \frac{\mathrm{i}}{2}\tilde{\rho}_{ac}\Omega_2 \\ \dot{\tilde{\rho}}_{ac} & = \frac{\mathrm{i}}{2}\tilde{\rho}_{ab}\Omega_2^* \end{array} \right. \tag{97}$$

where inhomogeneous dephasing and relaxation have been omitted, given the shortness of the pulse[4]. The first set of equations represents the coherent excitation of a two-level system. The second set describes the coupling of the optical coherence $\tilde{\rho}_{ab}$ and the Raman coherence $\tilde{\rho}_{ac}$. The solution of the latter set reads as:

$$\left\{ \begin{array}{ll} \tilde{\rho}_{ab}(t_2^{(+)}) & = \tilde{\rho}_{ab}(t_2^{(-)})\cos(\frac{1}{2}\int\Omega_2\mathrm{d}t) + \mathrm{i}\tilde{\rho}_{ac}(t_2^{(-)})\sin(\frac{1}{2}\int\Omega_2\mathrm{d}t) \\ \tilde{\rho}_{ac}(t_2^{(+)}) & = \tilde{\rho}_{ac}(t_2^{(-)})\cos(\frac{1}{2}\int\Omega_2\mathrm{d}t) + \mathrm{i}\tilde{\rho}_{ab}(t_2^{(-)})\sin(\frac{1}{2}\int\Omega_2\mathrm{d}t) \end{array} \right. \tag{98}$$

[4]With respect to Eq.26 we have modified the Rabi frequency definition in order to be consistent with the Bloch vector picture. Rabi frequency is now defined as $\mu_{ab}\mathcal{A}(\vec{r},t)/\hbar$ instead of $\mu_{ab}\mathcal{A}(\vec{r},t)/(2\hbar)$. With this definition the Bloch vector precession rate around axis Ou coincides with Ω. Numerical factors were simpler with the previous Ω definition.

A π-pulse optimizes the conversion of $\tilde{\rho}_{ab}$ into $\tilde{\rho}_{ac}$, leading to:

$$\tilde{\rho}_{ac}(t_2^{(+)}) = \mathrm{i}\tilde{\rho}_{ab}(t_2^{(-)}) = \mathrm{i}\tilde{\rho}_{ab}(\omega_{ab};\vec{r},t_1)\mathrm{e}^{(\mathrm{i}\Delta-\gamma_{ab})t_{12}} \tag{99}$$

Therefore the Raman coherence inherits the inhomogeneous dephasing that was accumulated by the optical coherence during interval t_{12}.

Total conversion of $\tilde{\rho}_{ab}$ into $\tilde{\rho}_{ac}$ means state $|b\rangle$ amplitude drops to 0. This is actually consistent with the two-level system evolution as described by Eq. 96.

We assume the Raman transition is not affected by inhomogeneous broadening and is resonantly excited by the driving fields in such a way that $\omega_{ac} = \omega_1 - \omega_2$. In other words, both $\tilde{\rho}_{ab}$ and $\tilde{\rho}_{cb}$ definitions refer to the same optical detuning $\Delta = \omega_{ab} - \omega_1 = \omega_{bc} - \omega_2$. The Raman coherence, evolving freely until excitation by the third pulse at t_3, reads as:

$$\tilde{\rho}_{ac}(t_3^{(-)}) = \mathrm{i}\tilde{\rho}_{ab}(\omega_{ab};\vec{r},t_1)\mathrm{e}^{(\mathrm{i}\Delta-\gamma_{ab})t_{12}-\gamma_{ac}t_{23}} \tag{100}$$

just before the pulse arrival. Once again, a π-pulse at frequency ω_1, exciting the system on the $a \rightarrow b$ transition, optimizes the conversion back to the optical coherence $\tilde{\rho}_{bc}$ that, just after the extinction of the pulse reads as:

$$\tilde{\rho}_{bc}(t_3^{(+)}) = \tilde{\rho}_{ab}(\omega_{ab};\vec{r},t_1)\mathrm{e}^{(\mathrm{i}\Delta-\gamma_{ab})t_{12}-\gamma_{ac}t_{23}} \tag{101}$$

Once the driving field is off, $\tilde{\rho}_{bc}$ evolves as: $\tilde{\rho}_{bc}(t) = \tilde{\rho}_{bc}(t_3^{(+)})\mathrm{e}^{(-\mathrm{i}\Delta-\gamma_{bc})(t-t_3)}$. The key point is that $\tilde{\rho}_{bc}$ phase factor evolves with opposite rate with respect to $\tilde{\rho}_{ab}$. Hence the inhomogeneous phase $\Delta(t_{12} - t + t_3)$ vanishes at $t_3 + t_{12}$, making the dipoles to radiate the tri-level echo on the $b \rightarrow c$ transition.

In the above discussion we implicitly assume the three pulses propagate along the same direction. As already noticed for two-pulse echoes, in more general conditions, we must take care that the "tilded" coherence definition depends on the relevant pulse wave vector direction. Let $\vec{k}_i$ denote the i^{th} pulse wave vector. Transformation to the rotating frame associated with the first two pulses leads to: $\tilde{\rho}_{ac} = \rho_{ac}\mathrm{e}^{\mathrm{i}(\omega_2-\omega_1)t-\mathrm{i}(\vec{k}_2-\vec{k}_1).\vec{r}}$ but the third pulse operates on a Raman coherence defined as: $\tilde{\rho}_{ac} = \rho_{ac}\mathrm{e}^{\mathrm{i}(\omega_2-\omega_1)t-\mathrm{i}(\vec{k}_2-\vec{k}_3).\vec{r}}$. To account for this transformation one can perform the substitution: $\tilde{\rho}_{ac}(t_3^{(-)}) \rightarrow \tilde{\rho}_{ac}(t_3^{(-)})\mathrm{e}^{\mathrm{i}(\vec{k}_3-\vec{k}_1)}$, which finally leads to:

$$\rho_{bc}(\omega_{ab};\vec{r},t) = \tilde{\rho}_{ab}(\omega_{ab};\vec{r},t_1)\mathrm{e}^{-\gamma_{ab}t_{12}-\gamma_{ab}t_{23}-\gamma_{ab}(t-t_3)}\times \\ \times\, \mathrm{e}^{-\mathrm{i}\omega_2 t-\mathrm{i}\Delta(t-t_3-t_{12})+\mathrm{i}(\vec{k}_3+\vec{k}_2-\vec{k}_1)} \tag{102}$$

Therefore the echo signal is emitted in direction $\vec{k}_3 + \vec{k}_2 - \vec{k}_1$. Then a phase matched signal can be emitted in a direction very different from that of the driving pulses. For instance, with $\vec{k}_3 = -\vec{k}_2 = -\vec{k}_1$ the echo signal is radiated backward, counterpropagating with the first pulse.

At first sight the three-level echo seems to represent a significant progress in our quest for phase reversal. As in two-pulse echo, the spectral phase is reversed but, unlike two-pulse echo, spatial phase can also be reversed, giving rise to backward signal emission. One also notice that the second pulse, despite of its large area, does not promote atoms to the upper level, avoiding amplification issues. Unfortunately the intense third pulse is coupled to $a \rightarrow b$ transition, strongly exciting the populated state $|a\rangle$ and massively promoting atoms to the upper electronic state.

We could be tempted to apply the third pulse to the empty transition $b \rightarrow c$ again instead of $a \rightarrow b$. However, this way, one cannot reverse the spectral phase. Indeed two successive π-pulses make a 2π rotation, which is no change at all. In other words, the second pulse builds ρ_{ac} from ρ_{ab} and, exciting $b \rightarrow c$ again, the third pulse turns back ρ_{ab} into ρ_{ac} without any phase inversion.

In conclusion, two out of the three signal recovery conditions are satisfied by the three-level echo. The third condition seems to be out of reach of the optical driving techniques. Non-optical procedures are thus considered.

7.3 Controlled reversible inhomogeneous broadening

It has been proposed to reverse the inhomogeneous spectral shift by inverting an external static electric field [23]. Actually the spectral shift must be totally controlled by an external field. In other words, the natural inhomogeneous broadening does not help. Instead, out of the inhomogeneously broadened medium, one has to select a group of atoms with the same transition frequency. This can be achieved by optically pumping the other atoms to an auxilliary shelving state. This works for instance in Pr^{3+}-doped crystals since three long lifetime sublevels are available in the electronic ground state. A non-uniform external field is then used to scatter the selected atoms over an artificially tailored bandwidth. The external non-uniform electric field is adjusted so that the engineered inhomogeneous broadening matches the bandwidth of the pulse to be stored. Provided that it is caused by linear Stark effect, the frequency shift can be reverted by inversion of the electric field. The procedure has been coined *Controlled reversible inhomogeneous*

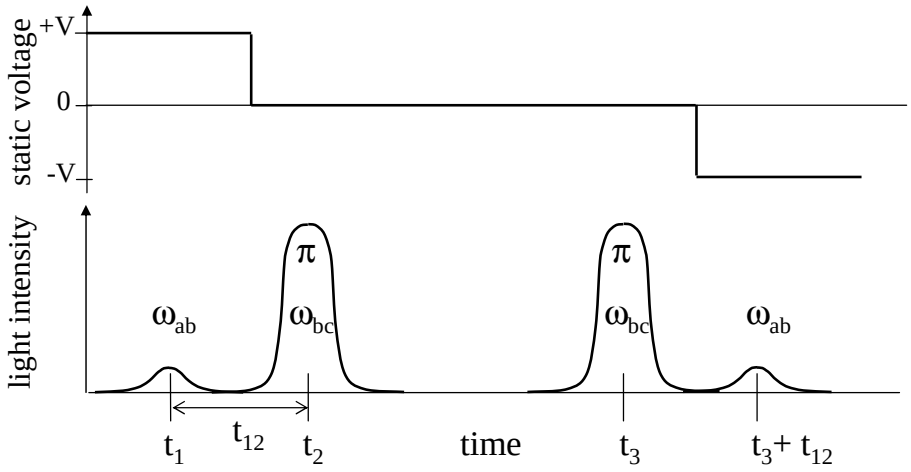

Figure 10: tri-level CRIB time-diagram. Inhomogeneous broadening is generated by Stark effect. The applied voltage polarity determines the sign of the spectral shift.

broadening [CRIB) by their instigators.

This procedure, first demonstrated in a two-level system [24, 25], should work best when combined with the tri-level echo (see Fig. 10). As discussed above, a narrow bandwidth group of atoms is first selected. They are prepared in state $|a\rangle$. The non-uniform electric field is switched on. The signal is directed to the absorbing medium at t_1. After signal extinction, the electric field is switched off and a π-pulse, tuned to the $b \rightarrow c$ transition, converts $\tilde{\rho}_{ab}$ into $\tilde{\rho}_{ac}$ at t_3. The recovery step contrasts significantly with the corresponding step in the conventional three-level echo. Instead of exciting the $a \rightarrow b$ transition, the π-pulse at t_3 is tuned again to the $b \rightarrow c$ empty transition, converting $\tilde{\rho}_{ac}$ back to $\tilde{\rho}_{ab}$. Then the electric field is turned back on, with inverted polarity. This way, $\tilde{\rho}_{ab}$ phase shift evolves at opposite rate and compensates for the previously accumulated phase shift. Atoms are rephased at time $t_3 + t_{12}$ and the echo signal is emitted.

The three criteria for total signal recall appear to be satisfied. Both spectral and spatial phase shift are reverted, and no atom is promoted to upper level by the π-pulses since both of them excite a transition between unpopulated states. However, the opacity of the absorbing material is altered by CRIB. Indeed, the available atoms, initially distributed over a narrow inter-

val δ, are spread by the external electric field over the memory bandwidth Δ_{mem}, which reduces the opacity by the factor δ/Δ_{mem}. One may wonder about the appropriate size of δ. Actually the initial width δ gives rise to an inhomogeneous phase shift that cannot be reverted. Because of this phase shift, the optical dipole available lifetime is limited to $\approx 1/\delta$, which must by far exceed the duration of the signal to be stored. As a consequence, the time-bandwidth product of the memory is limited by the quantity Δ_{mem}/δ, which is nothing but the inverse reduction factor of opacity. Therefore, it seems highly improbable to store anything but a single Fourier transform limited pulse, carrying one single information, with the CRIB technique.

8 Conclusion

We have reviewed two strategies for storing quantum light in a macroscopic ensemble of atoms. The discussion has been essentially conducted within the limits of the semi-classical picture. Essential features such as the retrieval efficiency can be addressed correctly within the frame of this picture. Moreover, this problem revives the interest in basic coherent light-matter interaction processes and sheds new light on them. However, a fully quantum analysis is needed to account for the entanglement of the atom ensemble, as resulting from coupling with quantum light. Despite of numerous efforts in this direction, a lot of work has still to be accomplished. Most of all, quantum memory for light has yet to be demonstrated experimentally in a solid. Both the theoretical obscurities and the experimental challenge make this field of research mostly attractive.

A Density operator

A.1 statistical mixing and quantum coherence

Let us consider a two level atom. Let $|a\rangle$ and $|b\rangle$ be the eigenstates of atomic hamiltonian with eigenvalues E_a and E_b. Let the atom be initially in state $|a\rangle$. Excitation by a light field prepares the atom in a superposition state $|\psi\rangle = a|a\rangle + b|b\rangle$. The notion of density operator clarifies the difference between a quantum state and a statistical mixture. The density operator is defined as:

$$\rho = |\psi\rangle\langle\psi| = \rho_m + \rho_q \tag{103}$$

where ρ_m and ρ_q respectively denote the diagonal and off-diagonal componants:

$$\begin{array}{rcl} \rho_m & = & |a|^2|a\rangle\langle a| + |b|^2|b\rangle\langle b| \\ \rho_q & = & ab^*|a\rangle\langle b| + a^*b|b\rangle\langle a| \end{array} \tag{104}$$

In an ensemble of N atoms, identically coupled to the field, the expectation values of the atom numbers in ground and excited states are repectively given by $N|a|^2$ and $N|b|^2$. The diagonal operator ρ_m accounts for this statistical mixture. However, ρ_m alone fails to describe the quantum properties. Those are expressed by the non-diagonal operator ρ_q. The off-diagonal elements $\langle a|\rho_q|b\rangle = \langle a|\rho|b\rangle = \rho_{ab}$ and $\langle b|\rho_q|a\rangle = \langle b|\rho|a\rangle = \rho_{ba}$ are named "quantum coherence".

To hold some physical meaning, the coherence has to be connected with the measure of an observable. The coherence associated with observable X can be defined as:

$$\begin{array}{rcl} C(X) & = & \mathrm{Tr}[(\rho - \rho_m)X] \\ & = & \langle a|(\rho - \rho_m)X|a\rangle + \langle b|(\rho - \rho_m)X|b\rangle \\ & = & \langle a|(\rho - \rho_m)|b\rangle\langle b|X|a\rangle + \langle b|(\rho - \rho_m)|a\rangle\langle a|X|b\rangle \end{array} \tag{105}$$

It appears that only observables with off-diagonal elements give access to quantum coherence. The macroscopic polarization density precisely owns this property.

A.2 Environment and relaxation

The density operator has helped us to introduce the notion of coherence. However, density operator is mostly known as a tool to account for the interaction of a quantum system with an environment, a bath with many degrees of freedom. This may be a radiation reservoir or a macroscopic material system. Connection with the environment usually leads to relaxation. So, interaction with radiation leads to decay from upper state to ground level by spontaneous emission. This affects the diagonal elements of the density operator. The off-diagonal elements are often more sensitive to coupling with environment and decay faster than population.

The notions of *partial trace* and *reduced density operator* can be introduced with the example of spontaneous emission. Let $|0_E\rangle$ and $|1_E\rangle$ respectively represent the 0- and 1-photon field state. In the product Hilbert state $\mathcal{H}_A \otimes \mathcal{H}_E$, the atom+field ensemble evolves according to unitary dynamics.

The state $|a\rangle \otimes |0_E\rangle$ remains unchanged since the atom is in the ground state. On the contrary the state $|b\rangle \otimes |0_E\rangle$ evolves to $|a\rangle \otimes |1_E\rangle$ with probability p during the time interval Δt. In other words, during the time interval Δt, the unitary operator U_{AE} transforms the compound state $|b\rangle \otimes |0_E\rangle$ into:

$$U_{AE}|b\rangle \otimes |0_E\rangle = \sqrt{1-p}\,|b\rangle \otimes |0_E\rangle + \sqrt{p}\,|a\rangle \otimes |1_E\rangle \tag{106}$$

This completes the unitary transform multiplication table, starting with a 0-photon state. Therefore, starting from an initial separable state:

$$|\psi\rangle \otimes |0_E\rangle = (a|a\rangle + b|b\rangle) \otimes |0_E\rangle \tag{107}$$

the atom-field system evolves to the entangled state:

$$|\Psi^{(1)}_{AE}\rangle = \left(a|a\rangle + b\sqrt{1-p}\,|b\rangle\right) \otimes |0_E\rangle + b\sqrt{p}\,|a\rangle \otimes |1_E\rangle \tag{108}$$

after one time interval Δt. Let ρ_{AE} denote the atom-field density operator. The expectation value of an observable O_A that only depends on atomic variables can be expressed as:

$$\langle O_A\rangle = \mathrm{Tr}_{\mathcal{H}_A\otimes\mathcal{H}_E}\left(O_A\rho_{AE}\right) = \mathrm{Tr}_{\mathcal{H}_E}\left(O_A\rho_{A(E)}\right) \tag{109}$$

where $\rho_{A(E)} = \mathrm{Tr}_{\mathcal{H}_E}(\rho_{AE})$represents the *reduced density operator*, resulting from *partial trace* of the total density operator over the field Hilbert space. Hence one just need the reduced density operator to determine any observable that only depends on the atomic parameters. In our simple model the field Hilbert space is spanned by the two states $|0_E\rangle$ and $|1_E\rangle$. Therefore, after one time interval Δt, the reduced density operator reads as:

$$\rho^{(1)}_{A(E)} = \mathrm{Tr}_{\mathcal{H}_E}\left(\rho^{(1)}_{AE}\right) = \langle 0_E|\Psi^{(1)}_{AE}\rangle\langle\Psi^{(1)}_{AE}|0_E\rangle + \langle 1_E|\Psi^{(1)}_{AE}\rangle\langle\Psi^{(1)}_{AE}|1_E\rangle, \tag{110}$$

which can be represented by the matrix:

$$\begin{aligned}\rho^{(1)}_{A(E)} &= \begin{bmatrix}\langle a|\rho^{(1)}_{A(E)}|a\rangle & \langle a|\rho^{(1)}_{A(E)}|b\rangle\\ \langle b|\rho^{(1)}_{A(E)}|a\rangle & \langle b|\rho^{(1)}_{A(E)}|b\rangle\end{bmatrix}\\ &= \begin{bmatrix}1-(1-p)\langle b|\rho^{(0)}_{A(E)}|b\rangle & \sqrt{1-p}\langle a|\rho^{(0)}_{A(E)}|b\rangle\\ \sqrt{1-p}\langle b|\rho^{(0)}_{A(E)}|a\rangle & (1-p)\langle b|\rho^{(0)}_{A(E)}|b\rangle\end{bmatrix}\end{aligned} \tag{111}$$

Let an evolution time interval t be described as a sequence of n elementary intervals of duration $\Delta t = t/n$. Assuming an iterative application of this transform, i.e. :

$$\rho_{A(E)}^{(m)} = \begin{bmatrix} 1-(1-p)\langle b|\rho_{A(E)}^{(m-1)}|b\rangle & \sqrt{1-p}\langle a|\rho_{A(E)}^{(m-1)}|b\rangle \\ \sqrt{1-p}\langle b|\rho_{A(E)}^{(m-1)}|a\rangle & (1-p)\langle b|\rho_{A(E)}^{(m-1)}|b\rangle \end{bmatrix}, \tag{112}$$

one finally obtains:

$$\rho_{A(E)}(t) = \begin{bmatrix} 1-\mathrm{e}^{-\gamma_b t}\langle b|\rho_{A(E)}(0)|b\rangle & \mathrm{e}^{-\gamma_b t/2}\langle a|\rho_{A(E)}(0)|b\rangle \\ \mathrm{e}^{-\gamma_b t/2}\langle b|\rho_{A(E)}(0)|a\rangle & \mathrm{e}^{-\gamma_b t}\langle b|\rho_{A(E)}(0)|b\rangle \end{bmatrix}, \tag{113}$$

where the ratio $p/\Delta t$ has been substituted with the spontaneous decay rate γ_b. This expresses the spontaneous emission effect on both populations and coherences. As expected upper level population decays to the ground level with rate γ_b. Less obviously, the coherence terms decay with rate $\gamma_b/2$. While the total density operator obeys unitary dynamics, the reduced operator appears to undergo non-unitary evolution.

Spontaneous emission is an inelastic process. Atomic excitation energy is transferred to the radiation field. However coherence relaxation may occur during elastic processes, the atom interacting with the environment without any population redistribution. Let an atom be coupled to a reservoir. Initially the atom+reservoir state reads as:

$$|\psi\rangle \otimes |\Xi\rangle = (a|a\rangle + b|b\rangle) \otimes |\Xi\rangle \tag{114}$$

where Ξ stands for the initial reservoir state. Let the compound system evolution be determined by the unitary operator $U(t)$ according to the following table:

$$|a\rangle \otimes |\Xi\rangle \overset{U(t)}{\rightarrow} |a\rangle \otimes |\Xi_a(t)\rangle \qquad |b\rangle \otimes |\Xi\rangle \overset{U(t)}{\rightarrow} |b\rangle \otimes |\Xi_b(t)\rangle \tag{115}$$

where:

$$\langle \Xi_a(t)|\Xi_a(t)\rangle = \langle \Xi_b(t)|\Xi_b(t)\rangle = \langle \Xi(t)|\Xi(t)\rangle = 1 \tag{116}$$

The atom stays in its initial state but the reservoir evolution depends on the atomic state. With the transformation table, the evolution of an arbitray compound state reads as:

$$|\psi\rangle \otimes |\Xi\rangle = (a|a\rangle + b|b\rangle) \otimes |\Xi\rangle \overset{U(t)}{\rightarrow} a|a\rangle \otimes |\Xi_a(t)\rangle + b|b\rangle \otimes |\Xi_b(t)\rangle \tag{117}$$

In the same way as in the spontaneous emission example, the system evolves to an entangled state. By performing the partial trace of the density operator over the reservoir states we then obtain the reduced density operator:

$$\rho(t) = \mathrm{Tr}\left[\rho_{at+\Xi}(t)\right] = \sum_{i_\Xi} \langle i_\Xi | \rho_{at+\Xi}(t) | i_\Xi \rangle \tag{118}$$

where states $|i_\Xi\rangle$ span the environment Hilbert space. In the basis set of vectors $|a\rangle, |b\rangle$, the reduced operator reads as:

$$\rho(t) = \begin{bmatrix} |a|^2 & ab^* \langle \Xi_b(t) | \Xi_a(t) \rangle \\ a^* b \langle \Xi_a(t) | \Xi_b(t) \rangle & |b|^2 \end{bmatrix} \tag{119}$$

The atomic coherence appears to be governed by the environment evolution. In general states $\Xi_a(t)\rangle$ and $\Xi_b(t)\rangle$ become more and more orthogonal as time elapse, gaining the orthogonality of their associated atomic states. This evolution can often be described as:

$$\langle \Xi_b(t) | \Xi_a(t) \rangle = \mathrm{e}^{-\gamma_{ab} t} \tag{120}$$

Spontaneous emission decay, combined with elastic relaxation, leads to the following general relation:

$$\gamma_{ab} \geq \gamma_b / 2 \tag{121}$$

B The Bloch vector

B.1 Connection with NMR

Developing the Nuclear Magnetic Resonance (NMR) theory, Felix Bloch describes the evolution of the magnetic moment operator expecting value and shows this quantity satisfies the equation of motion of a classical magnetic dipole. The Hamiltonian reads as $H = -\vec{M}.\vec{\mathcal{B}}$ where $\vec{\mathcal{B}}$ and $\vec{M}$ respectively represent the magnetic induction and the magnetic dipole moment. The latter is connected to the angular momentum $\vec{J}$ by $\vec{M} = \gamma\hbar\vec{J}$, where γ denotes the gyromagnetic ratio. From Schrödinger equation, and with the help of the commutation relations: $[J_x, J_y] = \mathrm{i}J_z$, $[J_z, J_x] = \mathrm{i}J_y$ and $[J_y, J_z] = \mathrm{i}J_x$, one easily shows that $\mathrm{d}\langle\vec{M}\rangle/\mathrm{d}t = -\gamma\vec{\mathcal{B}} \times \langle\vec{M}\rangle$. For instance, the equation of

$\langle M_x \rangle$ reads as:

$$\begin{aligned} \mathrm{i}\hbar\frac{\mathrm{d}\langle M_x\rangle}{\mathrm{d}t} &= \mathrm{i}\hbar\mathrm{Tr}\left(M_x \mathrm{d}\rho/\mathrm{d}t\right) = -\mathrm{Tr}\left(M_x\left[\vec{M}.\vec{\mathcal{B}},\rho\right]\right) \\ &= -\mathrm{Tr}\left\{M_x\left(\vec{M}.\vec{\mathcal{B}}\right)\rho\right\} + \mathrm{Tr}\left\{\rho\left(\vec{M}.\vec{\mathcal{B}}M_x\right)\right\} \\ &= -\mathcal{B}_y\left(\langle M_x M_y\rangle - \langle M_y M_x\rangle\right) - \mathcal{B}_z\left(\langle M_x M_z\rangle - \langle M_z M_x\rangle\right) \end{aligned} \tag{122}$$

The system evolves in $2J+1$ dimension Hilbert space, the state degeneracy being totally lifted by the applied magnetic field. The magnetic dipole moment operates in the Hilbert space, but the expectation value of its x, y, z components obey those equations of motion in *real space*.

Turning now to the two-level atoms, we know that the Hamiltonian can be expressed in terms of the Pauli matrices:

$$\sigma_1 = \begin{bmatrix} 0 & 1 \\ 1 & 0 \end{bmatrix}, \sigma_2 = \begin{bmatrix} 0 & -\mathrm{i} \\ \mathrm{i} & 0 \end{bmatrix}, \sigma_3 = \begin{bmatrix} 1 & 0 \\ 0 & -1 \end{bmatrix} \tag{123}$$

that can be put together to form the vector $\vec{\sigma}$. Hence the Hamiltonian of an atom interacting with a classical electromagnetic field reads as:

$$H_0 + eRE = \frac{1}{2}\hbar\omega_{ab}\sigma_3 + \mu_{ab}E\sigma_1 \tag{124}$$

where the state vector is expressed as: $|\psi\rangle = a|a\rangle + b|b\rangle = \begin{bmatrix} b \\ a \end{bmatrix}$

The Pauli matrices obey the same commutation rules as an angular momentum. More precisely, the spin operator defined as: $\vec{S} = \frac{1}{2}\vec{\sigma}$ obeys the commutation rules of a $J = 1/2$ angular momentum. Hence $\vec{\sigma}$ can be regarded as a magnetic moment. In the two-level atom Hamiltonian, the optical electric field and the level spacing respectively play the same role as the horizontal radio-frequency and the vertical static magnetic fields in NMR.

B.2 Bloch vector definition. Equation of motion

The Bloch vector $\vec{B}$ can be defined as the expectation value $\mathrm{Tr}\left(\rho\vec{\sigma}\right)$ of the Pauli operator. According to the equation of motion, the Bloch vector rapidly precesses around axis "3" at optical frequency ω_{ab}. The electric field oscillating at frequency ω_L along axis "1" can be broken up in two vectors rotating with opposite velocities ω_L and $-\omega_L$ within the plane orthogonal to axis "3". Only the electric field component at velocity ω_L close to ω_{ab} couples

efficiently to the Bloch vector. One neglects interaction with the other component rotating at $-\omega_L$. This is the rotating wave approximation.

In the frame of the rotating electric field component, the Bloch vector coordinates u, v, w are directly derived fom the definition $\vec{B} = \mathrm{Tr}\,(\rho\vec{\sigma})$ as:

$$\begin{cases} u &= \tilde{\rho}_{ab} + \tilde{\rho}_{ba} \\ v &= \mathrm{i}\,(\tilde{\rho}_{ba} - \tilde{\rho}_{ab}) \\ w &= \rho_{bb} - \rho_{aa} \end{cases} \tag{125}$$

The optical Bloch equation reads as[5]. :

$$\begin{cases} \dot{u} &= -\Delta v + \mathrm{Im}(\Omega) w - \gamma_{ab} u \\ \dot{v} &= \Delta u - \mathrm{Re}(\Omega) w - \gamma_{ab} v \\ \dot{w} &= -\mathrm{Im}(\Omega) u + \mathrm{Re}(\Omega) v - \gamma_b (1 + w) \end{cases} \tag{126}$$

In the same way as the motion of a magnetic moment immersed in a magnetic field, the Bloch equation can be written as:

$$\frac{\mathrm{d}\vec{B}}{\mathrm{d}t} = \vec{\beta} \times \vec{B} - \left.\frac{\mathrm{d}\vec{B}}{\mathrm{d}t}\right|_{relax} \tag{127}$$

where: $\vec{\beta} = \begin{cases} \mathrm{Re}(\Omega) \\ \mathrm{Im}(\Omega) \\ \Delta \end{cases}$, and $\left.\frac{\mathrm{d}\vec{B}}{\mathrm{d}t}\right|_{relax} = \begin{bmatrix} \gamma_{ab} & 0 & 0 \\ 0 & \gamma_{ab} & 0 \\ 0 & 0 & \gamma_b \end{bmatrix} \vec{B} + \begin{bmatrix} 0 \\ 0 \\ \gamma_b \end{bmatrix}$

Some geometrical properties come along with the precession form of the equation of motion:

- in the absence of relaxation, the length of $\vec{B}$ does not vary.
- if the system starts in a pure state, the length of $\vec{B}$ remains unity in the absence of relaxation.
- when $\vec{\beta}$ points to a fixed direction, $\vec{B}$ precesses around $\vec{\beta}$, at fixed angle. Projection of $\vec{B}$ on $\vec{\beta}$ direction is constant.

[5]In previous sections we had defined the Rabi frequency so as to get rid of useless numerical factors. In those sections the Bloch equation was expressed in terms of coherence and level population. From now on we modify the Rabi frequency definition in order to make the Bloch vector precession rate around axis Ou coincide with Ω. Rabi frequency is now defined as $\mu_{ab}\mathcal{A}(\vec{r},t)/\hbar$ instead of $\mu_{ab}\mathcal{A}(\vec{r},t)/(2\hbar)$.

- the driving vector $\vec{\beta}$, the Bloch vector $\vec{B}$ and the increase of $\vec{B}$ form a right-handed trihedron.

When atoms are resonantly excited by a fixed field, the Bloch vector rotates at angular frequency Ω in the plane orthogonal to $\vec{\beta}$. The resulting oscillation of w, representing the level population difference, is known as the *Rabi oscillation.*

References

[1] L.-M. Duan, M. Lukin, J. I. Cirac, P. Zoller, Long-distance quantum communication with atomic ensembles and linear optics, *Nature* **414** (2001) 413-418

[2] S.E. Harris, Electromagnetically Induced Transparency, *Physics Today* **50(7)**(1997) 36-42

[3] M. Fleischhauer, A. Imamoglu, and J. P. Marangos, Electromagnetically induced transparency: Optics in coherent media, *Rev. mod. Phys.* **77** (2005) 633

[4] L.V. Hau, S.E. Harris, Z. Dutton and C.H. Behroozi, Light speed reduction to 17 metres per second in an ultracold atomic gas, *Nature* **397** (1999) 594-598

[5] C. Liu, Z. Dutton, C.H. Behroozi and L.V. Hau, Observation of coherent optical information storage in an atomic medium using halted light pulses, *Nature* **409** (2001) 490-493

[6] D. F. Phillips, A. Fleischhauer, A. Mair, R. L. Walsworth, and M.D. Lukin, *Phys. Rev. Lett.* **86** (2001) 783

[7] N.V. Vitanov, M. Fleischhauer, B.W. Shore, and K. Bergmann, Coherent Manipulation of Atoms and Molecules by Sequential Pulses, *Adv. At. Mol. Opt. Phys.* **46** (2001) 55-190 (eds. B. Bederson, H. Walther, Academic Press)

[8] E. Arimondo, Coherent population trapping in laser spectroscopy, *Progress in Optics* **35** (1996) 257

[9] M. Fleischhauer and M. D. Lukin, Quantum memory for photons: Dark-state polaritons, *Phys. Rev. A* **65** (2002) 022314

[10] A. B. Matsko, Y. V. Rostovtsev, O. Kocharovskaya, A. S. Zibrov, and M. O. Scully, Nonadiabatic approach to quantum optical information storage *Phys. Rev. A* **64** (2001) 043809; A. S. Zibrov, A. B. Matsko, O. Kocharovskaya, Y. V. Rostovtsev, G. R. Welch, and M. O. Scully, Transporting and Time Reversing Light via Atomic Coherence, *Phys. Rev. Lett.* **88** (2002) 103601

[11] T. Chaneliere, D. N. Matsukevich, S. D. Jenkins, S. -Y. Lan, T. A. B. Kennedy and A. Kuzmich, Storage and retrieval of single photons transmitted between remote quantum memories, *Nature* **438** (2005) 833

[12] E. Kuznetsova, O. Kocharovskaya, Ph. Hemmer, and M. O. Scully, Atomic interference phenomena in solids with a long-lived spin coherence, *Phys. Rev. A* **66** (2002) 063802

[13] B.S. Ham, P.R. Hemmer, and M.S. Shahriar, Efficient Electromagnetically Induced Transparency in a Rare-Earth Doped Crystal, *Opt. Commun.* **144** (1997) 227-230

[14] Mark Phillips and Hailin Wang, Spin Coherence and Electromagnetically Induced Transparency via Exciton Correlations, *Phys. Rev. Lett.* **89** (2002) 186401

[15] M. Phillips, H. Wang, I. Rumyantsev, N. H. Kwong, R. Takayama, and R. Binder, Electromagnetically Induced Transparency in Semiconductors via Biexciton Coherence, *Phys. Rev. Lett.* **91** (2003) 183602

[16] P. R. Hemmer, A. V. Turukhin, M. S. Shahriar, J. A. Musser, Raman-excited spin coherences in nitrogen-vacancy color centers in diamond, *Opt. Lett.* **26** (2001) 361

[17] R. A. Akhmedzhanov, A. A. Bondartsev, L. A. Gushchin, N. A. Zharova, and A. G. Petrosyan, Electromagnetically Induced Transparency on Zeeman Sublevels in $Nd^{3+} : LaF_3$ Crystals, *JETP Lett.* **85** (2007) 389-92

[18] A. V. Turukhin, V.S. Sudarshanam, M.S. Shahriar, J.A. Musser, B.S. Ham, and P.R. Hemmer, Observation of Ultraslow and Stored Light Pulses in a Solid, *Phys. Rev. Lett.* **88** (2002) 023602

[19] J. J. Longdell, E. Fraval, M. J. Sellars, and N. B. Manson, Stopped Light with Storage Times Greater than One Second Using Electromagnetically Induced Transparency in a Solid, *Phys. Rev. Lett.* **95** (2005) 063601

[20] S. A. Moiseev and S. Kröll, Complete Reconstruction of the Quantum State of a Single-Photon Wave Packet Absorbed by a Doppler-Broadened Transition, *Phys. Rev. Lett.* **87** (2001) 173601

[21] N. Sangouard, C. Simon, M. Afzelius, and N. Gisin, Analysis of a quantum memory for photons based on controlled reversible inhomogeneous broadening *Phys. Rev. A* **75** (2007) 032327

[22] T. W. Mossberg, R. Kachru, S. R. Hartmann, and A. M. Flusberg, Echoes in gaseous media: A generalized theory of rephasing phenomena, *Phys. Rev. A* **20** (1979) 1976-1996

[23] M. Nilsson and S. Kröll, Solid state quantum memory using complete absorption and re-emission of photons by tailored and externally controlled inhomogeneous absorption profiles, *Opt. Commun.* **247** (2005) 393

[24] A. L. Alexander, J. J. Longdell, M. J. Sellars, and N. B. Manson, Photon Echoes Produced by Switching Electric Fields, *Phys. Rev. Lett.* **96** (2006) 043602

[25] G. Hétet, J. J. Longdell, A. L. Alexander, P. K. Lam, and M. J. Sellars, Gradient Echo Quantum Memory for Light using Two-level Atoms, arXiv:quant-ph/0612169